1-12-2024

Stick-Fixed Maneuver Points in Roll, Pitch, and Yaw and Associated Handling Qualities

Benjamin C. Moulton
Utah State University, ben.moulton@usu.edu

Troy A. Abraham
Utah State University, troy.abraham@usu.edu

Douglas F. Hunsaker
Utah State University, doug.hunsaker@usu.edu

Recommended Citation

Moulton, B. C., Abraham, T. A., and Hunsaker, D. F., "Stick-Fixed Maneuver Points in Roll, Pitch, and Yaw and Associated Handling Qualities," AIAA SciTech 2024 Forum, January 2024, AIAA-2024-2480 DOI: 10.2514/6.2024-2480

Stick-Fixed Maneuver Points in Roll, Pitch, and Yaw and Associated Handling Qualities

Benjamin C. Moulton*, Troy A. Abraham†, and Douglas F. Hunsaker‡
Utah State University, Logan, Utah 84322-4130

The stick-fixed pitch maneuver point is an important measure of aircraft longitudinal dynamic response and handling quality characteristics, and includes effects of both aerodynamic and inertia properties of the aircraft about the pitch axis. In the present work, the existence of stick-fixed roll and yaw maneuver points is demonstrated, which are determined from the lateral forces, moments, and inertial properties of the aircraft. These stick-fixed roll and yaw maneuver points are directly related to the predicted lateral handling qualities. Example results are included for several aircraft that demonstrate the importance of this parameter when predicting the dynamic response of the aircraft. A better understanding of stick-fixed roll, pitch, and yaw maneuver points can inform aircraft design during early stages to ensure adequate handling qualities for both longitudinal and lateral modes.

Nomenclature

a_{yy_b}, a_{zz_b}	=	pitch and yaw damping coefficients used to simplify mode approximations
a_{y_b}, a_{z_b}	=	body-fixed accelerations in the y_b and z_b axes
a_z	=	net flight-dynamic acceleration
B_a–B_j	=	coefficients used to determine roll and yaw dynamic margins
b_w	=	main wing span
CAP_{dr}, CAP_{sp}	=	Dutch roll and short-period control anticipation parameters
C_D	=	drag coefficient
C_{D_0}, $C_{D,L}$, C_{D,L^2}	=	drag coefficient parabolic terms
$C_{D,\bar{q}}$, C_{D,δ_e}	=	drag coefficient pitch damping and elevator control derivatives
C_L	=	lift coefficient
C_{L_0}	=	lift coefficient with $q = \alpha = \delta_e = 0$
$C_{L,\alpha}$, $C_{L,\bar{q}}$, C_{L,δ_e}	=	lift coefficient stability, pitch damping, and elevator control derivatives
$C_{L,\check{q}}$	=	change in lift coefficient with respect to dynamic pitch rate
C_ℓ	=	rolling moment coefficient
$C_{\ell_{np}}$	=	rolling moment coefficient about the neutral point
$C_{\ell,\beta}$, $C_{\ell,\bar{p}}$, $C_{\ell,\bar{r}}$	=	rolling moment coefficient stability, roll damping, and yaw damping derivatives
C_{ℓ,δ_a}, C_{ℓ,δ_r}	=	rolling moment coefficient aileron and rudder control derivatives
$C_{\check{\ell},\beta}$, $C_{\check{\ell},\check{r}}$	=	dynamic rolling moment coefficient stability and dynamic yaw rate derivatives
C_m	=	pitching moment coefficient
C_{m_0}	=	pitching moment coefficient with $q = \alpha = \delta_e = 0$
$C_{m_{np}}$	=	pitching moment coefficient about the neutral point
$C_{m,\alpha}$, $C_{m,\bar{q}}$, C_{m,δ_e}	=	pitching moment coefficient stability, pitch damping, and elevator control derivatives
C_n	=	yawing moment coefficient
$C_{n_{np}}$	=	yawing moment coefficient about the neutral point
$C_{n,\beta}$, $C_{n,\bar{p}}$, $C_{n,\bar{r}}$	=	yawing moment coefficient stability, roll damping, and yaw damping derivatives
C_{n,δ_a}, C_{n,δ_r}	=	yawing moment coefficient aileron and rudder control derivatives
$C_{\check{n},\beta}$, $C_{\check{n},\check{r}}$	=	dynamic yawing moment coefficient stability and dynamic yaw rate derivatives
C_S	=	side force coefficient

*PhD Student, Mechanical and Aerospace Engineering, 4130 Old Main Hill, AIAA Student Member
†PhD Student, Mechanical and Aerospace Engineering, 4130 Old Main Hill, AIAA Student Member
‡Associate Professor, Mechanical and Aerospace Engineering, 4130 Old Main Hill, AIAA Senior Member

$C_{S,\beta}$, $C_{S,\bar{p}}$, $C_{S,\bar{r}}$	=	side force coefficient stability, roll damping, and yaw damping derivatives
C_{S,δ_a}, C_{S,δ_r}	=	side force coefficient aileron and rudder control derivatives
C_W	=	weight coefficient
C_Y	=	stability axes side force coefficient
$C_{Y,\beta}$	=	stability axes side force coefficient stability derivative
C_θ, C_ϕ	=	cosine of elevation and bank angles
$\bar{c}_w$	=	main wing mean chord
D	=	drag force
D_o	=	drag force at the evaluated flight condition
F	=	force
F_{x_b}, F_{y_b}, F_{z_b}	=	force components in the x_b, y_b, and z_b axes
g	=	acceleration due to gravity
h_{mp_ℓ}, h_{np_ℓ}	=	y_a-distances up of the center of gravity to the roll maneuver and neutral points
h_{mp_m}, h_{np_m}	=	y_a-distances up of the center of gravity to the pitch maneuver and neutral points
I_{xx_b}, I_{yy_b}, I_{zz_b}	=	mass moments of inertia about the x_b, y_b, and z_b axes
$K_{\ell,\beta}$, $K_{\ell,\check{p}}$, $K_{\ell,\check{r}}$	=	changes in alternate rolling moment coefficient with respect to sideslip angle, dynamic roll rate, and dynamic yaw rate
$K_{m,\check{q}}$, $K_{m,\alpha}$, $K_{m,\check{\alpha}}$	=	changes in alternate pitching moment coefficient with respect to dynamic pitch rate, angle of attack, and dynamic time derivative of angle of attack
$K_{n,\beta}$, $K_{n,\check{p}}$, $K_{n,\check{r}}$	=	changes in alternate yawing moment coefficient with respect to sideslip angle, dynamic roll rate, and dynamic yaw rate
$K_{x,\alpha}$, $K_{x,\mu}$	=	changes in alternate x_b-force coefficient with respect to angle of attack and translational velocity
$K_{x,\alpha}$, $K_{x,\mu}$	=	changes in alternate x_b-force coefficient with respect to angle of attack and translational velocity
$K_{y,\beta}$, $K_{y,\check{r}}$	=	changes in alternate y_b-force coefficient with respect to sideslip angle and dynamic yaw rate
$K_{z,\alpha}$, $K_{z,\mu}$	=	changes in alternate z_b-force coefficient with respect to angle of attack and translational velocity
L	=	lift force
L_o	=	lift force at the evaluated flight condition
$L_{,\alpha}$	=	changes in lift force with respect to angle of attack
ℓ, m, n	=	rolling, pitching, and yawing moments about the x, y, and z axes
ℓ	=	rolling moment
ℓ_{np}	=	rolling moment about the neutral point
$\ell_{,\beta}$, $\ell_{,p}$, $\ell_{,r}$, $\ell_{,\check{r}}$	=	changes in rolling moment with respect to sideslip angle, roll rate, yaw rate, and dynamic yaw rate
l_{mp_m}, l_{np_m}	=	x_a-distances aft of the center of gravity to the pitch maneuver and neutral points
l_{mp_n}, l_{np_n}	=	x_a-distances aft of the center of gravity to the yaw maneuver and neutral points
l_{ref}	=	reference length used in traditional dimensionless moments
M	=	moment
m	=	pitching moment
m_{np}	=	pitching moment about the neutral point
$m_{,\dot{\alpha}}$	=	changes in pitching moment with respect to the time derivative of angle of attack
$m_{,\alpha}$, $m_{,q}$	=	changes in pitching moment with respect to angle of attack and pitch rate
n	=	yawing moment
n_N, n_S	=	normal and side-force load factors
n_{np}	=	yawing moment about the neutral point
$n_{,\beta}$, $n_{,p}$, $n_{,r}$, $n_{,\check{r}}$	=	changes in yawing moment with respect to sideslip angle, roll rate, yaw rate, and dynamic yaw rate
p, q, r	=	roll, pitch, and yaw rotation rates about the x_b, y_b, and z_b axes
$\bar{p}$, $\bar{q}$, $\bar{r}$	=	traditional dimensionless roll, pitch, and yaw rotation rates
$\check{q}$, $\check{r}$	=	dynamic pitch and yaw rotation rates
$\dot{q}_c$, $\dot{r}_c$	=	pitch and yaw angular acceleration limits

R_G	=	zero-wind glide ratio
R_{Dc}, R_{Dp}, R_{Ds}	=	Dutch roll mode coupling, phase-divergence, and stability ratios
r_p	=	pitch maneuver radius
R_{Pd}, R_{Pp}, R_{Ps}	=	phugoid mode pitch-damping, phase-divergence, and stability ratios
r_{xx_b}, r_{yy_b}, r_{zz_b}	=	roll, pitch, and yaw radii of gyration about the x_b, y_b, and z_b axes
S	=	side force
S_w	=	main wing area
S_θ, S_ϕ	=	sine of elevation and bank angles
s_{mp_ℓ}, s_{np_ℓ}	=	z_a-distances left of the center of gravity to the roll maneuver and neutral points
s_{mp_n}, s_{np_n}	=	z_a-distances left of the center of gravity to the yaw maneuver and neutral points
u, v, w	=	velocity components in the x_b, y_b, and z_b axes
$\dot{u}$, $\dot{v}$, $\dot{w}$	=	change in velocity components with respect to time in the x_b, y_b, and z_b axes
V	=	freestream velocity
V_o	=	freestream velocity at the evaluated flight condition
W	=	aircraft weight
x, y, z	=	wind coordinates relative to the center of gravity
x_a, y_a, z_a	=	aerodynamics coordinates relative to the center of gravity
x_b, y_b, z_b	=	aircraft body-fixed coordinates relative to the center of gravity
x_{cg}, y_{cg}, z_{cg}	=	coordinates of the center of gravity location
x_{mp_m}, x_{np_m}	=	x-locations of the pitch maneuver and neutral points in aerodynamics coordinates
x_{mp_n}, x_{np_n}	=	x-locations of the yaw maneuver and neutral points in aerodynamics coordinates
x_s, y_s, z_s	=	stability-axes coordinates relative to the center of gravity
$Y_{,\beta}$	=	change in stability axes side force with respect to sideslip angle
y_{mp_ℓ}, y_{np_ℓ}	=	y-locations of the roll maneuver and neutral points in aerodynamics coordinates
α	=	freestream angle of attack
β	=	freestream sideslip angle
δ_a, δ_e, δ_r	=	aileron, elevator, and rudder control surface deflections
ζ_{dr}, ζ_{ph}, $\zeta_{ph\,\mathrm{SLF}}$, ζ_{sp}	=	Dutch roll, general and steady-level flight phugoid, and short-period damping ratios
θ, ϕ	=	aircraft elevation and bank angles
θ_o, ϕ_o	=	aircraft elevation and bank angles at the evaluated flight condition
ρ	=	freestream air density
ς	=	freestream azimuth angle
σ_{dr}, σ_{ph}, $\sigma_{ph\,\mathrm{SLF}}$, σ_{sp}	=	Dutch roll, general and steady-level flight phugoid, and short-period damping rates
τ_{ro}	=	roll mode time constant
τ_{sl}	=	spiral mode doubling time constant
$\omega_{d_{dr}}$, $\omega_{d_{ph}}$, $\omega_{d_{ph\,\mathrm{SLF}}}$, $\omega_{d_{sp}}$	=	Dutch roll, general and steady-level flight phugoid, and short-period damped natural frequency
$\omega_{n_{dr}}$, $\omega_{n_{ph}}$, $\omega_{n_{ph\,\mathrm{SLF}}}$, $\omega_{n_{sp}}$	=	Dutch roll, general and steady-level flight phugoid, and short-period natural frequency

I. Introduction

Longitudinal and lateral handling-qualities* are a fundamental measure of the pilotability of an aircraft. Aircraft handling-quality limits have been chosen through extensive analysis of pilot opinion and dynamic characteristics of flight-tested aircraft [1], and have been studied and quantified extensively [2–14]. The evolving history of aircraft handling-qualities has detailed the extreme importance of the coupling between pilot opinion and aircraft design [3, 15–17]. Indeed some of the Wright brothers success has been attributed to the brothers' dual sharing of flight-test engineer and flight-test pilot roles [3]. However, the complicated effect of pilot opinion on aircraft controllability cannot be succinctly condensed.

Several groups have attacked the complexity of aircraft handling qualities in an attempt to understand the intricate phenomena of flight dynamics. Some groups have studied the effects on aircraft handling qualities of exacerbating maneuvers [18], design changes [9], and frequency-based pilot models [19]. Discussions [20–24] of and analytic

*In the literature there does not seem to be a difference in applied use of the terms flying qualities and handling qualities. For simplification the term handling qualities will be employed, given to mean the numeric ratings used to evaluate the dynamic response of an aircraft to a disturbance.

approximations [7, 25–36] to aircraft handling-qualities have been published in various flight-mechanics textbooks and technical reports. These approximations are frequently evaluated using the aircraft aerodynamic stability-derivatives data such as that reported by McRuer et al. [27], Teper [37], and Heffley and Jewell [38] for aircraft of varying roles. The approximate handling-quality relations are used to influence future aircraft design based on limits correlated from pilot opinion on flight-tested aircraft of similar role and capability.

Fundamental to the aircraft design process, the locations of the stick-fixed neutral point and stick-fixed maneuver point of an aircraft can have a significant effect on aircraft handling qualities. These points are typically derived considering *only* aircraft pitch dynamics. The purpose of the present paper is to develop and analyze roll and yaw analogs to the aircraft pitch stick-fixed neutral and maneuver points. Like those relating to pitch, the roll and yaw stick-fixed neutral and maneuver points can have a significant effect on handling qualities. The roll and yaw stick-fixed neutral and maneuver points are developed following steps similar to those used in the development of the pitch stick-fixed neutral [39] and maneuver [40, 41] points as presented by Phillips and Niewoehner. The derivation for these longitudinal characteristics are replicated in the present paper for completeness, following the process outlined by Phillips and Niewoehner [39–41].

In the present paper the approximate handling qualities relations developed by Phillips [42–46] and alternately presented by Hunsaker et al. [47] are rearranged to highlight the aircraft roll, pitch, and yaw static and dynamic margins. This process will involve the development of a Dutch-roll analog to the short-period control anticipation parameter (CAP) developed by Bihrle [48]. Key lessons can be drawn from the rearranged dynamic mode approximations for the aircraft design process. These steps will be taken to improve understanding of the underlying dynamical interactions between the aircraft static and dynamic margins and handling qualities.

A. Coordinate Frames

Prior to deriving the pitch static and dynamic margin, four coordinate frames are defined for use in the present paper. Only preliminary descriptions of each coordinate frame are presented, and further discussion on these coordinate frames is presented elsewhere [49].

The first is the aerodynamics coordinate frame. This coordinate frame consists of the origin located at the aircraft center of gravity, with the x_a-axis pointing out the tail, the y_a-axis pointing up and the z_a-axis pointing out the left wing, orthogonal to the x_a- and y_a-axes. This coordinate frame will be used to describe the location of the aircraft stick-fixed neutral and maneuver points.

The second is the aircraft body-fixed coordinate frame. This coordinate frame consists of the origin located at the aircraft center of gravity, with the x_b-axis pointing out the nose, the y_b-axis pointing out the right wing, and the z_b-axis pointing down, orthogonal to the x_b- and y_b-axes.

The third is the stability-axes coordinate frame. This coordinate frame consists of the origin located at the aircraft center of gravity, with the x_s-axis rotated in the $x_b z_b$-plane by some angle of attack α to align in the $x_b z_b$-plane with the freestream, the y_s-axis pointing out the right wing, and the z_s-axis pointing orthogonal to the x_s- and y_s-axes.

The fourth coordinate frame is the wind-axes coordinate frame. This coordinate frame consists of the origin located at the aircraft center of gravity, with the x-axis rotated in the $x_s y_s$-plane by some sideslip angle β to align exactly with the freestream, the y-axis rotated in the $x_s y_s$-plane by the sideslip angle, and the z-axis pointing orthogonal to the x- and y-axes. This coordinate frame will be used to describe wind-axes forces and moments D, S, L and ℓ, m, n, respectively.

B. Traditional Pitch Stick-Fixed Neutral Point

The pitch stick-fixed neutral point is defined as the location on the aircraft where the change in the pitching moment with respect to angle of attack is zero. The angle of attack is defined as the angle made between the fuselage reference line and the freestream as seen normal to the aircraft $x_b z_b$ plane, shown in Fig. 1.

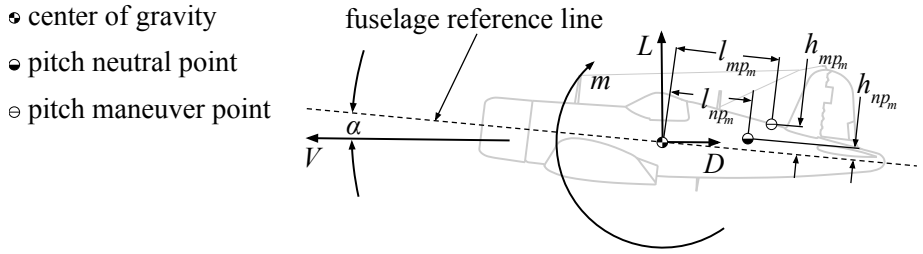

Fig. 1 Pitch stick-fixed neutral and maneuver points sign convention.

Summing the moments about the y_b axis at the pitch stick-fixed neutral point, which is the aerodynamic center of the aircraft, it can be found that

$$m_{np} = m + l_{np_m}\left(L\cos\alpha + D\sin\alpha\right) + h_{np_m}\left(L\sin\alpha - D\cos\alpha\right) \tag{1}$$

where α is the angle of attack, L is the lift force, D is the drag force, m is the pitching moment, and l_{np_m} and h_{np_m} are the length and height measured in the aircraft body-fixed $x_b z_b$-plane between the center of gravity and the pitch stick-fixed neutral point, respectively. Note, though the forces and moments are given in the wind-axes coordinate frame, the lengths presented in Eq. (1) and shown in Fig. 1 are in the aerodynamics coordinate frame. Thus a pitch stick-fixed neutral point aft and above the aircraft center of gravity will have positive length and height measures.

An aerodynamic force F or longitudinal moment M is traditionally written in dimensionless form as

$$C_F = \frac{F}{\frac{1}{2}\rho V^2 S_w}, \quad C_M = \frac{M}{\frac{1}{2}\rho V^2 S_w l_{ref}} \tag{2}$$

where ρ is the freestream air density, V is the freestream velocity, S_w is the main-wing area, and l_{ref} is a reference length (traditionally $\bar{c}_w$ is for longitudinal moments). Assuming α is small, the offset height h_{np_m} is negligible, and D is small compared to L, Eq. (1) can be rewritten in dimensionless form as

$$C_{m_{np}} \cong C_m + \frac{l_{np_m}}{\bar{c}_w} C_L \tag{3}$$

Taking the derivative with respect to angle of attack, and recalling $\frac{\partial C_{m_{np}}}{\partial \alpha} = C_{m_{np},\alpha} = 0$:

$$C_{m_{np},\alpha} = 0 \cong C_{m,\alpha} + \frac{l_{np_m}}{\bar{c}_w} C_{L,\alpha} \tag{4}$$

which can be rearranged to form the traditional relation for the pitch static margin [39]

$$\frac{l_{np_m}}{\bar{c}_w} \cong -\frac{C_{m,\alpha}}{C_{L,\alpha}} \tag{5}$$

Note, the main-wing mean chord used in Eq. (5) could have been any other reference length as shown in Eq. (2). This variability can cause confusion when referencing a "rule of thumb" for the pitch static margin if the reference length is not explicitly given. Equation (5) can be written in dimensional form as

$$l_{np_m} \cong -\frac{m_{,\alpha}}{L_{,\alpha}} \tag{6}$$

While Eq. (5) is a valuable measure of the pitch static stability of an aircraft, this measure does not include dynamic effects. As noted by Phillips and Niewoehner, any rule of thumb for the pitch static margin in the aircraft design process can be extremely misleading with respect to the dynamic response of the aircraft [40]. The pitch static margin relation can be used to define a pitch stick-fixed maneuver point and dynamic margin, which include pitch dynamics as a measure of the pitch dynamic stability of an aircraft.

C. Pitch Rate Related to Normal Acceleration

A relationship can be established between the aircraft normal load factor and pitch rate for use in deriving the pitch dynamic margin. The normal load factor on an aircraft is the ratio of lift L produced to the weight W of the aircraft:

$$n_N \equiv \frac{L}{W} \tag{7}$$

The normal acceleration on an aircraft is a function of this load factor, as [41]

$$a_z = (n_N - 1)g \tag{8}$$

where g is the acceleration due to gravity. Unity is subtracted from the normal load factor n_N to account for the acceleration of the aircraft due to gravity. Thus, a_z is a net flight-dynamic acceleration. This normal acceleration can be related to the aircraft tangential velocity V and radius r_p in a pitch up maneuver through centripetal acceleration, as

$$a_z = \frac{V^2}{r_p} \tag{9}$$

The pitch rate of the aircraft in a pitch maneuver is the angular distance traveled by the aircraft divided by the time taken to travel this distance. This pitch rate q can be found as

$$q = \frac{2\pi}{2\pi\frac{r_p}{V}} = \frac{V}{r_p} \tag{10}$$

which can be related to the load factor as

$$q = \frac{V}{r_p} = \frac{a_z}{V} = \frac{(n_N - 1)g}{V} \tag{11}$$

This leads to the development of what has been termed the *dynamic pitch rate* $\breve{q}$ which is related to the normal load factor as [41]

$$\breve{q} = \frac{Vq}{g} = \frac{2V^2\bar{q}}{g\bar{c}_w} = \frac{a_z}{g} = (n_N - 1) \tag{12}$$

where $\bar{q}$ is the traditional dimensionless pitch rate $\bar{q} = \frac{q\bar{c}_w}{2V}$. The relation shown here for the dynamic pitch rate was originally suggested by Phillips and Niewoehner [40, 41], and will be used to develop the pitch dynamic margin.

D. Traditional Pitch Maneuver Margin

A general uncoupled aerodynamic model will be used for the following maneuver point developments. This model is linear, with the exception of a single term for the quadratic dependence of drag on lift. This model is

$$\begin{aligned}
C_L &= C_{L_0} + C_{L,\alpha}\alpha + C_{L,\bar{q}}\bar{q} + C_{L,\delta_e}\delta_e \\
C_S &= C_{S,\beta}\beta + C_{S,\bar{p}}\bar{p} + C_{S,\bar{r}}\bar{r} + C_{S,\delta_a}\delta_a + C_{S,\delta_r}\delta_r \\
C_D &= C_{D_0} + C_{D,L}C_{L_1} + C_{D,L^2}C_{L_1}^2 + C_{D,\bar{q}}\bar{q} + C_{D,\delta_e}\delta_e \\
C_\ell &= C_{\ell,\beta}\beta + C_{\ell,\bar{p}}\bar{p} + C_{\ell,\bar{r}}\bar{r} + C_{\ell,\delta_a}\delta_a + C_{\ell,\delta_r}\delta_r \\
C_m &= C_{m_0} + C_{m,\alpha}\alpha + C_{m,\bar{q}}\bar{q} + C_{m,\delta_e}\delta_e \\
C_n &= C_{n,\beta}\beta + C_{n,\bar{p}}\bar{p} + C_{n,\bar{r}}\bar{r} + C_{n,\delta_a}\delta_a + C_{n,\delta_r}\delta_r
\end{aligned} \tag{13}$$

where

$$C_{L_1} \equiv C_{L_0} + C_{L,\alpha}\alpha \tag{14}$$

While this model is simple, it is sufficient for developing the subsequent relationships.

The dimensionless pitch rate $\bar{q}$ can be replaced in the general aerodynamic model in Eq. (13) with a dynamic relation to loading in the normal axis, resulting in the relationship

$$\bar{q} = (n_N - 1)\frac{g\bar{c}_w}{2V^2} \tag{15}$$

Additionally replacing the lift coefficient with the corresponding normal load factor and weight as in Eq. (7) in steady-level flight (zero pitching moment) and neglecting drag results in the trim equations:

$$\begin{aligned} n_N C_W &= C_{L_0} + C_{L,\alpha}\alpha + C_{L,\bar{q}}(n_N - 1)\frac{g\bar{c}_w}{2V^2} + C_{L,\delta_e}\delta_e \\ 0 &= C_{m_0} + C_{m,\alpha}\alpha + C_{m,\bar{q}}(n_N - 1)\frac{g\bar{c}_w}{2V^2} + C_{m,\delta_e}\delta_e \end{aligned} \tag{16}$$

These equations can be rearranged with aerodynamic angles and control surface deflections on the left, as

$$\begin{aligned} C_{L,\alpha}\alpha + C_{L,\delta_e}\delta_e &= n_N C_W - C_{L_0} - C_{L,\bar{q}}(n_N - 1)\frac{g\bar{c}_w}{2V^2} \\ C_{m,\alpha}\alpha + C_{m,\delta_e}\delta_e &= -C_{m_0} - C_{m,\bar{q}}(n_N - 1)\frac{g\bar{c}_w}{2V^2} \end{aligned} \tag{17}$$

From which are obtained the following equations

$$\begin{bmatrix} C_{L,\alpha} & C_{L,\delta_e} \\ C_{m,\alpha} & C_{m,\delta_e} \end{bmatrix} \begin{bmatrix} \alpha \\ \delta_e \end{bmatrix} = \begin{bmatrix} n_N C_W - C_{L_0} - C_{L,\bar{q}}(n_N - 1)\frac{g\bar{c}_w}{2V^2} \\ -C_{m_0} - C_{m,\bar{q}}(n_N - 1)\frac{g\bar{c}_w}{2V^2} \end{bmatrix} \tag{18}$$

The left hand side matrix can be inverted to find

$$\begin{bmatrix} \alpha \\ \delta_e \end{bmatrix} = \frac{1}{C_{L,\alpha}C_{m,\delta_e} - C_{L,\delta_e}C_{m,\alpha}} \begin{bmatrix} C_{m,\delta_e} & -C_{L,\delta_e} \\ -C_{m,\alpha} & C_{L,\alpha} \end{bmatrix} \begin{bmatrix} n_N C_W - C_{L_0} - C_{L,\bar{q}}(n_N - 1)\frac{g\bar{c}_w}{2V^2} \\ -C_{m_0} - C_{m,\bar{q}}(n_N - 1)\frac{g\bar{c}_w}{2V^2} \end{bmatrix} \tag{19}$$

or expanded as

$$\begin{bmatrix} \alpha \\ \delta_e \end{bmatrix} = \frac{1}{C_{L,\alpha}C_{m,\delta_e} - C_{L,\delta_e}C_{m,\alpha}} \begin{bmatrix} \left(n_N C_W - C_{L_0}\right) + C_{L,\delta_e}C_{m_0}C_{m,\delta_e} + \left(C_{L,\delta_e}C_{m,\bar{q}} - C_{L,\bar{q}}C_{m,\delta_e}\right)(n_N - 1)\frac{g\bar{c}_w}{2V^2} \\ -\left(n_N C_W - C_{L_0}\right)C_{m,\alpha} - C_{L,\alpha}C_{m_0} - \left(C_{L,\alpha}C_{m,\bar{q}} - C_{L,\bar{q}}C_{m,\alpha}\right)(n_N - 1)\frac{g\bar{c}_w}{2V^2} \end{bmatrix} \tag{20}$$

The control surface deflection equation can now be differentiated with respect to the n_N load factor term to find

$$\frac{\partial\delta_e}{\partial n_N} = -\frac{C_W C_{m,\alpha} + \left(C_{L,\alpha}C_{m,\bar{q}} - C_{L,\bar{q}}C_{m,\alpha}\right)\frac{g\bar{c}_w}{2V^2}}{C_{L,\alpha}C_{m,\delta_e} - C_{L,\delta_e}C_{m,\alpha}} \tag{21}$$

Using the pitch static margin in Eq. (5) and rearranging:

$$\frac{\partial\delta_e}{\partial n_N} = -\frac{C_W - C_{L,\bar{q}}\frac{g\bar{c}_w}{2V^2}}{C_{m,\delta_e} + C_{L,\delta_e}\frac{l_{np_m}}{\bar{c}_w}}\left(\frac{C_{m,\bar{q}}\frac{g\bar{c}_w}{2V^2}}{C_W - C_{L,\bar{q}}\frac{g\bar{c}_w}{2V^2}} - \frac{l_{np_m}}{\bar{c}_w}\right) \tag{22}$$

Note, the location of the pitch neutral point is defined as the difference in position between the aircraft center of gravity and pitch stick-fixed neutral point, shown in Fig. 1, as

$$l_{np_m} = x_{np_m} - x_{cg} \tag{23}$$

where x_{np_m} is the x-location of the pitch stick-fixed neutral point, and x_{cg} is the x-location of the center of gravity, both in the aerodynamics coordinate frame. Thus

$$\frac{\partial\delta_e}{\partial n_N} = -\frac{C_W - C_{L,q}\frac{g}{V}}{C_{m,\delta_e} + C_{L,\delta_e}\left(\frac{x_{np_m}}{\bar{c}_w} - \frac{x_{cg}}{\bar{c}_w}\right)}\left(\frac{C_{m,q}\frac{g}{V}}{C_W - C_{L,q}\frac{g}{V}} - \frac{x_{np_m}}{\bar{c}_w} + \frac{x_{cg}}{\bar{c}_w}\right) \tag{24}$$

The pitch maneuver point is where an infinitesimal change in elevator deflection causes an infinite change in load factor [25, 36, 50]. As shown in the above equation, there is some point at which if the cg is located the elevator angle to normal acceleration value is 0. This is the *pitch maneuver point* (and knowing typically $C_W \gg C_{L,\breve{q}}$), [40, 41]

$$x_{mp_m} = x_{np_m} - \frac{\bar{c}_w C_{m,q}\frac{g}{V}}{C_W - C_{L,q}\frac{g}{V}} = x_{np_m} - \frac{m_{,q}\frac{g}{V}}{W} = x_{cg} - \frac{m_{,\alpha}}{L_{,\alpha}} - \frac{m_{,q}\frac{g}{V}}{W} \tag{25}$$

as in other developments [25, 26, 31, 32, 36, 50]. Note, the pitch maneuver point x_{mp_m} is defined in the aerodynamic coordinate frame. The location of the pitch maneuver point relative to the center of gravity is estimated from [40, 41]

$$l_{mp_m} = -\frac{m_{,\alpha}}{L_{,\alpha}} - \frac{m_{,q}\frac{g}{V}}{W} \tag{26}$$

resulting in the pitch dynamic margin [40, 41]

$$\frac{l_{mp_m}}{r_{yy_b}} = -\frac{m_{,\alpha}}{L_{,\alpha} r_{yy_b}} - \frac{m_{,q}\frac{g}{V}}{W r_{yy_b}} \tag{27}$$

where the pitch radius-of-gyration is

$$r_{yy_b} = \sqrt{\frac{g I_{yy_b}}{W}} \tag{28}$$

The decision to nondimensionalize the longitudinal dynamic margin by the pitch radius-of-gyration will be justified later in the present paper. This dynamical relation was noted by Cook [51] and Phillips and Niewoehner [40, 41] and was shown to directly correlate to the aircraft short-period mode CAP. Indeed, Bihrle established, as noted by Phillips and Niewoehner, the pitch dynamic margin to be related to a pitch angular acceleration $\dot{q}_c$ as [40, 41, 48]

$$\frac{l_{mp_m}}{r_{yy_b}} \geq \frac{\dot{q}_c}{g/r_{yy_b}} \tag{29}$$

The pitch angular acceleration term can be directly correlated to a pitch-acceleration-sensitivity limit, which is the short-period CAP [41]. The purpose of the CAP is to mitigate pilot-induced oscillations [48]. However, pilot-induced oscillations are affected not only by short-period characteristics, but Dutch-roll oscillations as well [52]. The authors emphasize that the Dutch-roll mode is the lateral equivalent to the longitudinal short-period mode. The purpose of the present paper is to develop roll and yaw equivalents to the pitch characteristics developed in previous work. These roll and yaw characteristics are developed using the understanding and methodology presented in the pitch static margin and dynamic margin derivations culminating in Eqs. (5) and (27).

II. Roll and Yaw Stick-Fixed Neutral Points

The pitch stick-fixed neutral point is traditionally the location about which the change in the pitching moment of the aircraft with respect to angle of attack is zero, and has been used in aircraft design to inform on pitch static stability. The derivation of the pitch neutral point results in the familiar Eq. (5). As will be shown here, roll and yaw stick-fixed neutral points can similarly be defined, which can inform on aircraft roll and yaw static stability.

A. Roll Stick-Fixed Neutral Point

The roll stick-fixed neutral point can be determined using the sum of moments about the aircraft body-fixed x_b-axis. This sum of moments depends on the lift and side forces, as well as the angle the freestream makes about the x_b-axis. This angle can be considered a freestream analog to the orientation bank angle. The freestream azimuth angle is defined as the angle made between the fuselage reference line and the freestream as seen from the nose of the aircraft, shown in Fig. 2. Note, this angle inherently depends on the freestream angle of attack and sideslip angle.

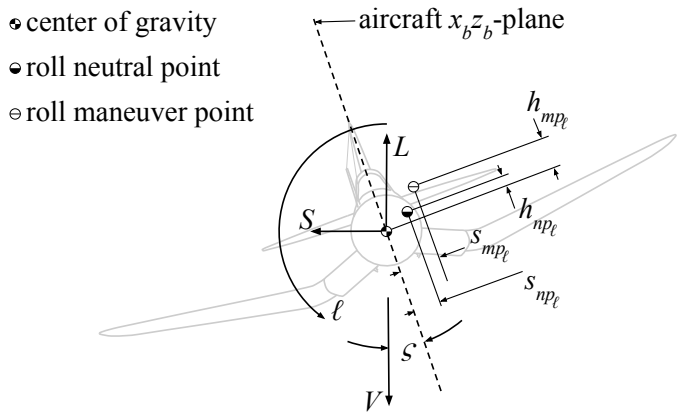

Fig. 2 Roll stick-fixed neutral and maneuver points sign convention.

Knowing the freestream angle of attack $\alpha = \tan^{-1}\left(\frac{w}{u}\right)$ and analytic sideslip angle $\beta = \tan^{-1}\left(\frac{v}{u}\right)$, the freestream azimuth angle is defined as

$$\varsigma = \tan^{-1}\left(\frac{v}{w}\right) = \tan^{-1}\left(\frac{\tan\beta}{\tan\alpha}\right) \tag{30}$$

The freestream azimuth angle is measured between the positive z_b-axis and freestream velocity vector dotted onto the $y_b z_b$-plane. Summing the moments about the x_b-axis at the roll stick-fixed neutral point results in

$$\ell_{np} = \ell + h_{np_\ell}\left(-S\cos\varsigma + L\sin\varsigma\right) + s_{np_\ell}\left(-L\cos\varsigma - S\sin\varsigma\right) \tag{31}$$

Assuming ς is small ($S \cong Y$, $Y\cos\varsigma >> L\sin\varsigma$), and side length s_{np_ℓ} is negligible ($s_{np_\ell} = 0$ for a symmetric aircraft), Eq. (31) can be rewritten in dimensionless form as

$$C_{\ell_{np}} \cong C_\ell + \frac{h_{np_\ell}}{b_w}\left(-C_Y\right) \tag{32}$$

Taking the derivative with respect to sideslip angle, and defining $\frac{\partial C_{\ell_{np}}}{\partial\beta} = C_{\ell_{np},\beta} = 0$ at the roll neutral point,

$$C_{\ell_{np},\beta} = 0 \cong C_{\ell,\beta} + \frac{h_{np_\ell}}{b_w}\left(-C_{Y,\beta}\right) \tag{33}$$

Which can be rearranged to form the relation for the roll static margin

$$\frac{h_{np_\ell}}{b_w} \cong \frac{C_{\ell,\beta}}{C_{Y,\beta}} \tag{34}$$

Equation (34) can be written in dimensional form as

$$h_{np_\ell} \cong \frac{\ell_{,\beta}}{Y_{,\beta}} \tag{35}$$

By definition a statically stable aircraft has a negative roll stability derivative and a negative side-force slope (i.e. $C_{\ell,\beta} < 0$, $C_{Y,\beta} < 0$). Thus, similar to the pitch static margin expressed in Eq. (5), the roll static margin defined in (34) indicates roll static stability when $h_{np_\ell} > 0$.

B. Yaw Stick-Fixed Neutral Point

The yaw stick-fixed neutral point can be determined using the sum of moments about the aircraft body-fixed z_b-axis. This sum of moments depends on the side and drag forces, as well as the angle the freestream makes about the z_b-axis. This angle is the sideslip angle, which is the angle made between the fuselage reference line and the freestream as seen from above the aircraft, shown in Fig. 3.

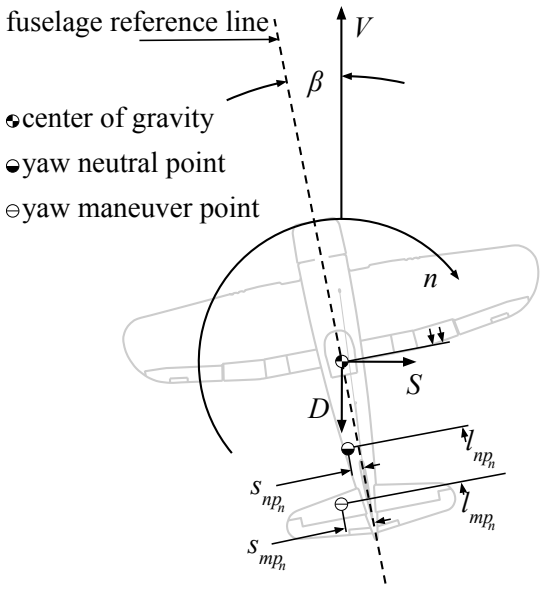

Fig. 3 Yaw stick-fixed neutral and maneuver points sign convention.

Summing the moments about the z_b-axis at the yaw stick-fixed neutral point results in

$$n_{np} = n + l_{np_n}\left(S\cos\beta - D\sin\beta\right) + s_{np_n}\left(-S\sin\beta - D\cos\beta\right) \tag{36}$$

Assuming β is small ($S \cong Y$), the offset distance s_{np_n} is negligible ($s_{np_n} = 0$ for a symmetric aircraft), and $C_D\beta << 1$, Eq. (36) can be written in dimensionless form as

$$C_{n_{np}} \cong C_n + \frac{l_{np_n}}{b_w} C_Y \tag{37}$$

Taking the derivative with respect to sideslip angle, and defining $\frac{\partial C_{n_{np}}}{\partial \beta} = C_{\ell_{np},\beta} = 0$,

$$C_{n_{np},\beta} = 0 \cong C_{n,\beta} + \frac{l_{np_n}}{b_w} C_{Y,\beta} \tag{38}$$

Which can be rearranged to form the relation for the yaw static margin

$$\frac{l_{np_n}}{b_w} \cong -\frac{C_{n,\beta}}{C_{Y,\beta}} \tag{39}$$

Equation (39) can be written in dimensional form as

$$l_{np_n} \cong -\frac{n_{,\beta}}{Y_{,\beta}} \tag{40}$$

By definition a statically stable aircraft has a positive yaw stability derivative and a negative side-force slope (i.e. $C_{n,\beta} > 0$, $C_{Y,\beta} < 0$). Thus, similar to the pitch static margin expressed in Eq. (5) and the roll static margin expressed in Eq. (34), the yaw static margin defined in (39) indicates static roll stability when $l_{np_n} > 0$.

Note, three separate stick-fixed neutral points have been defined in the present paper: the traditional pitch stick-fixed neutral point in Eq. (6), a roll stick-fixed neutral point in Eq. (35), and a yaw stick-fixed neutral point in Eq. (40). These equations must not be misunderstood to define three separate aerodynamic centers. In truth there is only one aerodynamic center: the cause for the three individual stick-fixed neutral points developed in the present paper stems from the assumptions and approximations used in the development of each stick-fixed neutral point. For example, in the yaw stick-fixed neutral point derivation it was assumed the yawing moment is only dependant on sideslip angle, aerodynamic angles were small, etc.

Using these assumptions decoupled the interdependence of roll, pitch, and yaw. This may seem to be an extremely limiting assumption. However, the utility of three separate static margins (and three corresponding dynamic margins) will be demonstrated later in the present paper where dynamic mode approximations are developed.

III. Roll and Yaw Stick-Fixed Maneuver Margins

The relations for the roll static margin in Eq. (34) and yaw static margin in Eq. (39) can be used to develop the roll and yaw dynamic margins. Just as the traditional pitch maneuver margin can be developed from the pitch trim equations as shown in Eq. (26), it will be shown that the roll and yaw maneuver points can be obtained from the lateral trim equations. These lateral trim equations will depend on the side-force load factor, as the pitch trim equations depended on the normal load factor. Similar to the pitch dynamic margin derivation, a relation between the side-force load factor and yawing rate will first be developed.

A. Dynamic Rates Related to Normal and Side Accelerations

From the rigid-body equations of motion, the general body-fixed translational acceleration for an aircraft can be found as [53]

$$\begin{bmatrix} \dot{u} \\ \dot{v} \\ \dot{w} \end{bmatrix} = \frac{g}{W} \begin{bmatrix} F_{x_b} \\ F_{y_b} \\ F_{z_b} \end{bmatrix} + g \begin{bmatrix} -S_\theta \\ S_\phi C_\theta \\ C_\phi C_\theta \end{bmatrix} + \begin{bmatrix} rv - qw \\ pw - ru \\ qu - pv \end{bmatrix} \tag{41}$$

where ϕ denotes the bank angle and θ denotes the elevation angle. The relationship presented in Subsection I.C could have been derived from the third equation in Eq. (41). The third equation in Eq. (41) can be rearranged as (Note $\frac{g}{W} = \frac{1}{m}$)

$$-\frac{F_{z_b}}{mg} - C_\phi C_\theta = \frac{qu - pv - \dot{w}}{g} \tag{42}$$

For steady ($\dot{w} = 0$), purely-longitudinal motion ($p = v = 0$), assuming small angles ($C_\theta \cong 1$, $C_\phi \cong 1$, $u \cong V$), this equation can be simplified to

$$\breve{q} = \frac{Vq}{g} = \frac{2V^2\bar{q}}{g\bar{c}_w} = -\frac{a_{z_b}}{g} - 1 = n_N - 1 \tag{43}$$

where a_{z_b} is the net acceleration in the body-fixed z_b-axis, thus resulting in the same relationship developed previously in Eq. (12) [41]. A similar approach can be taken with the second equation in Eq. (41), rearranging as

$$\frac{F_{y_b}}{mg} + S_\phi C_\theta = \frac{ru - pw + \dot{v}}{g} \tag{44}$$

For steady ($\dot{v} = 0$), purely-lateral motion ($w = 0$), assuming small angles ($S_\phi \cong \phi$, $C_\theta \cong 1$, $u \cong V$), this equation can be simplified to

$$\breve{r} = \frac{Vr}{g} = \frac{2V^2\bar{r}}{gb_w} = \frac{a_{y_b}}{g} = n_S + \phi \tag{45}$$

where a_{y_b} is the net acceleration in the body-fixed y_b-axis. The relationship between the pitch rate and normal load factor through the dynamic pitch rate $\breve{q}$ given in Eq. (12) and alternately derived in Eq. (43) was originally presented by Phillips and Niewoehner [40, 41]. The dimensionless form of the dynamic pitch rate was applied to the roll and yaw rates by Phillips [54] and further justified by Hunsaker et. al. [47] as a more dynamics-appropriate dimensionless form for the aircraft rotation rates. This can readily be seen in Eqs. (43) and (45), which give direct relations between the normal load factor n_N and pitch rate q, and the side-force load factor n_S and yaw rate r. As with the pitch dynamic margin derivation, this yaw relation will be used to derive the roll and yaw dynamic margins.

B. Roll and Yaw Maneuver Margins Derivation

The dimensionless yaw rate $\bar{r}$ can be related to the side-force load factor as

$$\bar{r} = (n_S + \phi)\frac{gb_w}{2V^2} \tag{46}$$

In the lateral force and moment equations in the aerodynamic model given in Eq. (13) the dimensionless yaw rate $\bar{r}$ terms can be replaced with the terms given in Eq. (46). Replacing the side-force coefficient with corresponding

side-force load factor and weight coefficient and setting the moments to zero results in the lateral trim equations:

$$\begin{aligned} n_S C_W &= C_{S,\beta}\beta + C_{S,\bar{p}}\bar{p} + C_{S,\bar{r}}(n_S+\phi)\frac{gb_w}{2V^2} + C_{S,\delta_a}\delta_a + C_{S,\delta_r}\delta_r \\ 0 &= C_{\ell,\beta}\beta + C_{\ell,\bar{p}}\bar{p} + C_{\ell,\bar{r}}(n_S+\phi)\frac{gb_w}{2V^2} + C_{\ell,\delta_a}\delta_a + C_{\ell,\delta_r}\delta_r \\ 0 &= C_{n,\beta}\beta + C_{n,\bar{p}}\bar{p} + C_{n,\bar{r}}(n_S+\phi)\frac{gb_w}{2V^2} + C_{n,\delta_a}\delta_a + C_{n,\delta_r}\delta_r \end{aligned} \tag{47}$$

The lateral trim equations can be rearranged with aerodynamic angles and control surface deflections on the left, as

$$\begin{aligned} C_{S,\beta}\beta + C_{S,\delta_a}\delta_a + C_{S,\delta_r}\delta_r &= n_S C_W - C_{S,\bar{p}}\bar{p} - C_{S,\bar{r}}(n_S+\phi)\frac{gb_w}{2V^2} \\ C_{\ell,\beta}\beta + C_{\ell,\delta_a}\delta_a + C_{\ell,\delta_r}\delta_r &= -C_{\ell,\bar{p}}\bar{p} - C_{\ell,\bar{r}}(n_S+\phi)\frac{gb_w}{2V^2} \\ C_{n,\beta}\beta + C_{n,\delta_a}\delta_a + C_{n,\delta_r}\delta_r &= -C_{n,\bar{p}}\bar{p} - C_{n,\bar{r}}(n_S+\phi)\frac{gb_w}{2V^2} \end{aligned} \tag{48}$$

or

$$\begin{bmatrix} C_{S,\beta} & C_{S,\delta_a} & C_{S,\delta_r} \\ C_{\ell,\beta} & C_{\ell,\delta_a} & C_{\ell,\delta_r} \\ C_{n,\beta} & C_{n,\delta_a} & C_{n,\delta_r} \end{bmatrix} \begin{bmatrix} \beta \\ \delta_a \\ \delta_r \end{bmatrix} = \begin{bmatrix} n_S C_W - C_{S,\bar{p}}\bar{p} - C_{S,\bar{r}}(n_S+\phi)\frac{gb_w}{2V^2} \\ -C_{\ell,\bar{p}}\bar{p} - C_{\ell,\bar{r}}(n_S+\phi)\frac{gb_w}{2V^2} \\ -C_{n,\bar{p}}\bar{p} - C_{n,\bar{r}}(n_S+\phi)\frac{gb_w}{2V^2} \end{bmatrix} \tag{49}$$

The left-hand-side matrix can be inverted to the right-hand side to find

$$\begin{bmatrix} \beta \\ \delta_a \\ \delta_r \end{bmatrix} = \frac{1}{B_j}\begin{bmatrix} B_a & B_b & B_c \\ B_d & B_e & B_f \\ B_g & B_h & B_i \end{bmatrix} \begin{bmatrix} n_S C_W - C_{S,\bar{p}}\bar{p} - C_{S,\bar{r}}(n_S+\phi)\frac{gb_w}{2V^2} \\ -C_{\ell,\bar{p}}\bar{p} - C_{\ell,\bar{r}}(n_S+\phi)\frac{gb_w}{2V^2} \\ -C_{n,\bar{p}}\bar{p} - C_{n,\bar{r}}(n_S+\phi)\frac{gb_w}{2V^2} \end{bmatrix} \tag{50}$$

where

$$B_a = C_{\ell,\delta_a}C_{n,\delta_r} - C_{\ell,\delta_r}C_{n,\delta_a} \tag{51}$$
$$B_b = -(C_{S,\delta_a}C_{n,\delta_r} - C_{S,\delta_r}C_{n,\delta_a}) \tag{52}$$
$$B_c = C_{S,\delta_a}C_{\ell,\delta_r} - C_{S,\delta_r}C_{\ell,\delta_a} \tag{53}$$
$$B_d = -(C_{\ell,\beta}C_{n,\delta_r} - C_{\ell,\delta_r}C_{n,\beta}) \tag{54}$$
$$B_e = C_{S,\beta}C_{n,\delta_r} - C_{S,\delta_r}C_{n,\beta} \tag{55}$$
$$B_f = -(C_{S,\beta}C_{\ell,\delta_r} - C_{S,\delta_r}C_{\ell,\beta}) \tag{56}$$
$$B_g = C_{\ell,\beta}C_{n,\delta_a} - C_{\ell,\delta_a}C_{n,\beta} \tag{57}$$
$$B_h = -(C_{S,\beta}C_{n,\delta_a} - C_{S,\delta_a}C_{n,\beta}) \tag{58}$$
$$B_i = C_{S,\beta}C_{\ell,\delta_a} - C_{S,\delta_a}C_{\ell,\beta} \tag{59}$$
$$B_j = C_{S,\beta}B_a + C_{S,\delta_a}B_d + C_{S,\delta_r}B_g \tag{60}$$

or in expanded form

$$\begin{bmatrix} \beta \\ \delta_a \\ \delta_r \end{bmatrix} = \frac{(n_S+\phi)}{B_j}\begin{bmatrix} B_a C_W - \frac{gb_w}{2V^2}\left(B_a C_{S,\bar{r}} + B_b C_{\ell,\bar{r}} + B_c C_{n,\bar{r}}\right) \\ B_d C_W - \frac{gb_w}{2V^2}\left(B_d C_{S,\bar{r}} + B_e C_{\ell,\bar{r}} + B_f C_{n,\bar{r}}\right) \\ B_g C_W - \frac{gb_w}{2V^2}\left(B_g C_{S,\bar{r}} + B_h C_{\ell,\bar{r}} + B_i C_{n,\bar{r}}\right) \end{bmatrix} - \frac{\phi C_W}{B_j}\begin{bmatrix} B_a \\ B_d \\ B_g \end{bmatrix} - \frac{1}{B_j}\begin{bmatrix} B_a C_{S,\bar{p}} + B_b C_{\ell,\bar{p}} + B_c C_{n,\bar{p}} \\ B_d C_{S,\bar{p}} + B_e C_{\ell,\bar{p}} + B_f C_{n,\bar{p}} \\ B_g C_{S,\bar{p}} + B_h C_{\ell,\bar{p}} + B_i C_{n,\bar{p}} \end{bmatrix}\bar{p} \tag{61}$$

Note, the dimensionless body-fixed roll rate $\bar{p}$ is independent of the side-force load factor for purely lateral flight. Thus, $\frac{\partial \bar{p}}{\partial n_S} = 0$. The control surface deflection equations in Eq. (61) can be differentiated with respect to the n_S acceleration term as

$$\begin{aligned} \frac{\partial \delta_a}{\partial n_S} &= \frac{B_d C_W - \frac{gb_w}{2V^2}\left(B_d C_{S,\bar{r}} + B_e C_{\ell,\bar{r}} + B_f C_{n,\bar{r}}\right)}{B_j} \\ \frac{\partial \delta_r}{\partial n_S} &= \frac{B_g C_W - \frac{gb_w}{2V^2}\left(B_g C_{S,\bar{r}} + B_h C_{\ell,\bar{r}} + B_i C_{n,\bar{r}}\right)}{B_j} \end{aligned} \tag{62}$$

Using the roll static margin in Eq. (34) and yaw static margin in Eq. (39) with Eqs. (51)–(60), $C_{S,\beta}$ terms in the numerator and denominator can be cancelled. These steps result in the equations:

$$\frac{\partial \delta_a}{\partial n_S} = \frac{-(\frac{h_{np_\ell}}{b_w} C_{n,\delta_r} + C_{\ell,\delta_r} \frac{l_{np_n}}{b_w}) \left(C_W - \frac{g b_w}{2V^2} C_{S,\bar{r}} \right) - \frac{g b_w}{2V^2} \left((C_{n,\delta_r} + C_{S,\delta_r} \frac{l_{np_n}}{b_w}) C_{\ell,\bar{r}} - (C_{\ell,\delta_r} - C_{S,\delta_r} \frac{h_{np_\ell}}{b_w}) C_{n,\bar{r}} \right)}{(C_{\ell,\delta_a} C_{n,\delta_r} - C_{\ell,\delta_r} C_{n,\delta_a}) - C_{S,\delta_a} (\frac{h_{np_\ell}}{b_w} C_{n,\delta_r} + C_{\ell,\delta_r} \frac{l_{np_n}}{b_w}) + C_{S,\delta_r} (\frac{h_{np_\ell}}{b_w} C_{n,\delta_a} + C_{\ell,\delta_a} \frac{l_{np_n}}{b_w})}$$

$$\frac{\partial \delta_r}{\partial n_S} = \frac{(\frac{h_{np_\ell}}{b_w} C_{n,\delta_a} + C_{\ell,\delta_a} \frac{l_{np_n}}{b_w}) \left(C_W - \frac{g b_w}{2V^2} C_{S,\bar{r}} \right) - \frac{g b_w}{2V^2} \left(-(C_{n,\delta_a} + C_{S,\delta_a} \frac{l_{np_n}}{b_w}) C_{\ell,\bar{r}} + (C_{\ell,\delta_a} - C_{S,\delta_a} \frac{h_{np_\ell}}{b_w}) C_{n,\bar{r}} \right)}{(C_{\ell,\delta_a} C_{n,\delta_r} - C_{\ell,\delta_r} C_{n,\delta_a}) - C_{S,\delta_a} (\frac{h_{np_\ell}}{b_w} C_{n,\delta_r} + C_{\ell,\delta_r} \frac{l_{np_n}}{b_w}) + C_{S,\delta_r} (\frac{h_{np_\ell}}{b_w} C_{n,\delta_a} + C_{\ell,\delta_a} \frac{l_{np_n}}{b_w})} \tag{63}$$

We will now define some point at which infinitesimal changes in the aileron and rudder deflection angles cause an infinite change in the side-force load factor. This is the *lateral maneuver point*. The numerators in Eq. (63) can be set equal to zero, and rearranged to solve for the roll and yaw static margins. This results in the relationships (bringing the static margins to the right hand side):

$$0 = -\frac{C_{\ell,r} \frac{g}{V}}{C_W - C_{S,r} \frac{g}{V}} - \frac{h_{np_\ell}}{b_w} \tag{64}$$

$$0 = \frac{C_{n,r} \frac{g}{V}}{C_W - C_{S,r} \frac{g}{V}} - \frac{l_{np_n}}{b_w} \tag{65}$$

Recall the location of the stick-fixed neutral point is defined as the difference in position between the aircraft center of gravity and stick-fixed neutral point, shown in Figs. 2 and 3, as

$$h_{np_\ell} = y_{np_\ell} - y_{cg} \tag{66}$$

$$l_{np_n} = x_{np_n} - x_{cg} \tag{67}$$

where y_{np_ℓ} and x_{np_n} are the y_a- and x_a-locations of the roll and yaw stick-fixed neutral points, respectively, and x_{cg} and y_{cg} are the x_a- and y_a-locations of the aircraft center of gravity, all in the aerodynamics coordinate frame. Thus

$$0 = -\frac{C_{\ell,r} \frac{g}{V}}{C_W - C_{S,r} \frac{g}{V}} - \frac{y_{np_\ell}}{b_w} + \frac{y_{cg}}{b_w} \tag{68}$$

$$0 = \frac{C_{n,r} \frac{g}{V}}{C_W - C_{S,r} \frac{g}{V}} - \frac{x_{np_n}}{b_w} + \frac{x_{cg}}{b_w} \tag{69}$$

Defining the maneuver points (and knowing typically $C_W \gg C_{S,\check{r}} = C_{S,r} \frac{g}{V}$),

$$y_{mp_\ell} = y_{np_\ell} + \frac{b_w C_{\ell,r} \frac{g}{V}}{C_W - C_{S,r} \frac{g}{V}} = y_{np_\ell} + \frac{\ell_{,r} \frac{g}{V}}{W} = y_{cg} + \frac{\ell_{,\beta}}{Y_{,\beta}} + \frac{\ell_{,r} \frac{g}{V}}{W} \tag{70}$$

$$x_{mp_n} = x_{np_n} - \frac{b_w C_{n,r} \frac{g}{V}}{C_W - C_{S,r} \frac{g}{V}} = x_{np_n} - \frac{n_{,r} \frac{g}{V}}{W} = x_{cg} - \frac{n_{,\beta}}{Y_{,\beta}} - \frac{n_{,r} \frac{g}{V}}{W} \tag{71}$$

where roll maneuver point y_{mp_ℓ} and yaw maneuver point x_{mp_n} are defined in the aerodynamics coordinate frame. The location of the maneuver points relative to the center of gravity are estimated from

$$h_{mp_\ell} = \frac{\ell_{,\beta}}{Y_{,\beta}} + \frac{\ell_{,r} \frac{g}{V}}{W} \tag{72}$$

$$l_{mp_n} = -\frac{n_{,\beta}}{Y_{,\beta}} - \frac{n_{,r} \frac{g}{V}}{W} \tag{73}$$

resulting in the roll and yaw dynamic margins

$$\frac{h_{mp_\ell}}{r_{xx_b}} = \frac{C_{\check{\ell},\beta}}{C_{Y,\beta}} + \frac{C_{\check{\ell},\check{r}}}{C_W} = \frac{\ell_{,\beta}}{Y_{,\beta} r_{xx_b}} + \frac{\ell_{,\check{r}}}{W r_{xx_b}} \tag{74}$$

$$\frac{l_{mp_n}}{r_{zz_b}} = -\frac{C_{\check{n},\beta}}{C_{Y,\beta}} - \frac{C_{\check{n},\check{r}}}{C_W} = -\frac{n_{,\beta}}{Y_{,\beta} r_{zz_b}} - \frac{n_{,\check{r}}}{W r_{zz_b}} \tag{75}$$

where the roll and yaw radii-of-gyration are

$$r_{xx_b} = \sqrt{\frac{gI_{xx_b}}{W}} \tag{76}$$

$$r_{zz_b} = \sqrt{\frac{gI_{zz_b}}{W}} \tag{77}$$

The decision to nondimensionalize the roll and yaw dynamic margins by the roll and yaw radii-of-gyration is due to the dynamic nature of the radii of gyration length scales being more appropriate for these measures of dynamic properties [40]. Indeed, it will be shown later that the radii of gyration naturally form as denominators to the roll and yaw maneuver margins when developing approximations for the lateral dynamic modes. Static and dynamic margins have now been developed for roll, pitch, and yaw. These relationships can be used to demonstrate how the aircraft closed-form dynamic-mode approximations developed by Phillips [42–46] and alternately presented by Hunsaker et. al. [47] are affected by the roll, pitch, and yaw dynamic margins.

IV. Dynamic Mode Approximations and Handling Qualities

Approximations to the dynamic modes are frequently used to evaluate the handling qualities of an aircraft design. Although the dynamic-mode approximations are not typically formulated in terms of neutral points or maneuver points, these approximations will be expressed here in terms of the roll, pitch, and yaw neutral and maneuver margins (or roll, pitch, and yaw static and dynamic margins). As will be shown, such a formulation can shed significant light on how these parameters are related to final handling qualities. The dynamic mode approximations are given following for the short-period, phugoid, roll, spiral, and Dutch-roll modes formulated using the roll, pitch, and yaw static margins given in Eqs. (34), (5), and (39) and dynamic margins given in Eqs. (27), and (74) and (75). The change in these dynamic mode approximations due to dynamic margins are presented for typical representatives of four classes [55] of aircraft: a general aviation aircraft (Class I, Navion from Teper [37]), a mid-size business jet (Class II, Lockheed Jetstar from Heffley [38]), a large commercial airliner (Class III, Boeing 747 from Heffley [38]), and a fighter aircraft (Class IV, F-94A from Blakelock [30]). Further analysis is dedicated to the Dutch-roll mode and a proposed Dutch-roll control-anticipation parameter.

A. Short-Period Mode

The dynamic properties generally used to measure the controllability of the short-period mode are the CAP [48] and damping ratio. The CAP can be determined from the closed-form equation of the natural frequency $\omega_{n_{sp}}$ as [42]

$$\text{CAP}_{sp} = \frac{\omega_{n_{sp}}^2}{\partial n_N/\partial\alpha} \approx \frac{\omega_{n_{sp}}^2}{C_{L,\alpha}/C_W} = \frac{g l_{mp_m}}{r_{yy_b}^2} \tag{78}$$

and the damping ratio (derived in the appendix, subsection A.A) becomes

$$\zeta_{sp} = -\frac{1}{2}\sqrt{\frac{L_{,\alpha}}{I_{yy_b} l_{mp_m}}}\left(\frac{m_{,\dot{\alpha}}}{L_{,\alpha}} + a_{yy_b}\right) \tag{79}$$

where

$$a_{yy_b} = \frac{m_{,q}}{L_{,\alpha}} - \frac{r_{yy_b}^2}{V_o} \tag{80}$$

Most studies of dynamic mode approximations acknowledge the dependence of the CAP on the stick-fixed pitch dynamic margin [51, 56–59], and Cook [51] and Phillips and Niewoehner [40, 59] have quantified an approximate relationship between the stick-fixed pitch dynamic margin and CAP. Equations (78)–(80) show the dependence of the short-period dynamic properties on the pitch dynamic margin l_{mp_m}. As the pitch dynamic margin increases, the CAP increases and the damping ratio decreases.

These effects can be seen in Fig. 5 for typical representatives of four classes [55] of aircraft in different flight phases: a general aviation aircraft (Class I, Phase B, Navion from Teper [37]), a mid-size business jet (Class II, Phase C, Lockheed Jetstar from Heffley [38]), a large commercial airliner (Class III, Phase C, Boeing 747 from Heffley [38]),

and a fighter aircraft (Class IV, Phase A, F-94A from Blakelock [30]). The 'exact' markers on Fig. 4 denote the mode properties as determined from an eigen analysis of the linearized system of longitudinal equations. As the pitch dynamic margin decreases on each aircraft, at some point the short-period mode eigenvalues become non-oscillatory. The linearized eigen analysis results previous to this point are not reported.

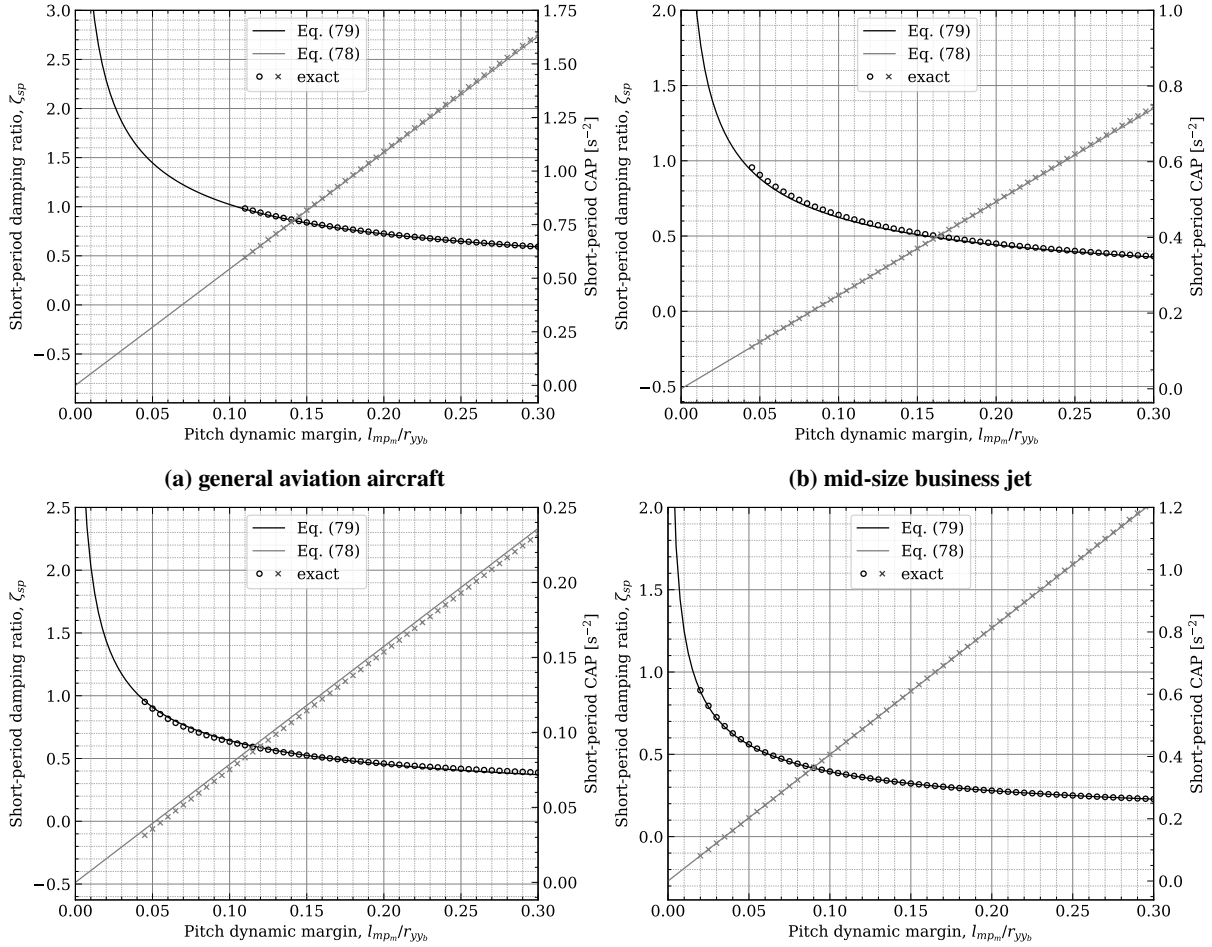

(a) general aviation aircraft

(b) mid-size business jet

(c) large commercial airliner

(d) fighter aircraft

Fig. 4 Change in short-period damping ratio and CAP with pitch dynamic margin.

The plots in Fig. 4 indicate the general trend mentioned above for various aircraft in different flight phases. But what are the handling qualities of an aircraft as a result of changing pitch dynamic margin? The change in aircraft handling qualities as a function of the short-period mode properties is shown in Fig. 5 for the same four aircraft and flight phases described above. The arrow heads on Fig. 5 denote the direction of increasing pitch dynamic margin in increments of 5%.

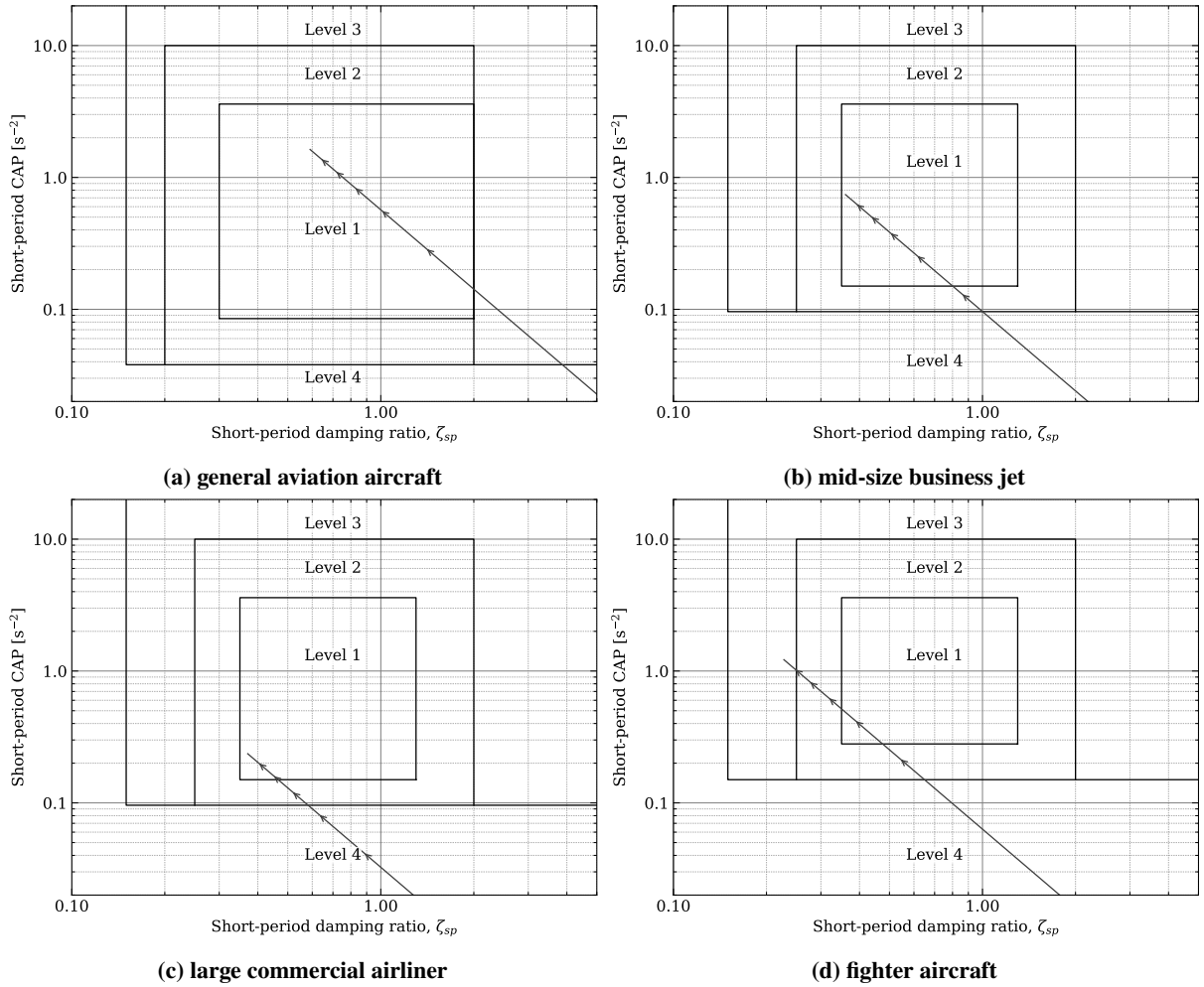

(a) general aviation aircraft

(b) mid-size business jet

(c) large commercial airliner

(d) fighter aircraft

Fig. 5 Change in short-period mode handling qualities with pitch dynamic margin, arrows indicating the direction of increasing pitch dynamic margin in increments of 5%.

Two important principles are shown in Fig. 5. First, across various aircraft increasing the pitch dynamic margin will generally result in improved short-period mode handling qualities. Rather than a steady improvement (i.e. from level 4 to level 3, level 3 to level 2, etc.), however, the handling qualities may skip levels (i.e. level 4 to level 3, level 3 to level 1 as in Fig. 5a). Second, There can be such a thing as too much pitch stability! This is shown in Fig. 5d for the fighter aircraft (and suggested in Figs. 5b and 5c for the mid-size business jet and the large commercial airliner). There is a point ($\frac{l_{mp_m}}{r_{yy_b}} \approx 18\%$) at which increasing the pitch dynamic margin results in deteriorating handling qualities for the fighter aircraft. This suggests that for a desired level of handling qualities the approximate short-period mode properties can be used to set upper and lower bounds on acceptable locations for the aircraft center of gravity.

B. Phugoid Mode

The mode property generally used to measure acceptable handling qualities of the phugoid mode is the damping ratio. The damping ratio is a combination of the damping rate and the natural frequency. The phugoid damping ratio (derived in the appendix, subsection A.B) is found to be

$$\zeta_{ph} = \frac{D_o}{W}\sqrt{\frac{Wl_{mp_m}}{2L_o l_{np_m}}} + \frac{g}{V_o}\sqrt{\frac{L_o l_{np_m}}{2Wl^3_{mp_m}}}a_{yy_b} \tag{81}$$

For steady level flight, assuming small angles, ($\phi_o = 0$, $\cos\theta_o \approx 1$, $L_o = W$, $R_G = \frac{L_o}{D_o}$) the phugoid damping rate is

$$\sigma_{ph\,\mathrm{SLF}} = \frac{g}{V_o}\left[\frac{1}{R_G} + \frac{g}{V_o}\frac{l_{np_m}}{l_{mp_m}^2}a_{yy_b}\right] \tag{82}$$

The phugoid natural frequency in steady level flight is found to be

$$\omega_{n_{ph\,\mathrm{SLF}}} = \frac{g}{V_o}\sqrt{\frac{2l_{np_m}}{l_{mp_m}}} \tag{83}$$

and the phugoid damping ratio in steady level flight is

$$\zeta_{ph\,\mathrm{SLF}} = \frac{1}{R_G}\sqrt{\frac{l_{mp_m}}{2l_{np_m}}} + \frac{g}{V_o}\sqrt{\frac{l_{np_m}}{2l_{mp_m}^3}}a_{yy_b} \tag{84}$$

It has commonly been stated that more aerodynamically efficient aircraft have lower phugoid mode damping [43, 56–58, 60–62]. This effect can be directly seen in Eqs. (82)–(84). An aircraft with greater glide ratio (the dominant term in the equation) will have a lower phugoid damping rate.

However, most dynamic analyses define the phugoid natural frequency and damping ratio to be of the form [56, 57, 60–65]

$$\omega_{n_{ph}} = \sqrt{2}\frac{g}{V_o} \tag{85}$$

$$\zeta_{ph} = \frac{1}{\sqrt{2}R_G} \tag{86}$$

neglecting the effects due to pitch static and dynamic margins, described above in Eqs. (82) and (83). It has been acknowledged that the phugoid damping ratio depends on the pitch static margin, but this relationship was not quantified [56]. Similar effects due to the radius of gyration r_{yy_b} are neglected in other formulations, and as such the inertial damping effect on the phugoid mode is neglected. Notably, these approximations had not changed over the course of nearly 50 years.

Note that $m_{,q}$ and a_{yy_b} are typically negative, and R_G, g, and V_o are typically positive. The interplay between the pitch dynamic margin and phugoid damping ratio demonstrates the effect that, while counter-intuitive, a slight shifting aft of the center of gravity may result in increased damping of the phugoid mode. This can be seen in Fig. 6 for typical representatives of four classes of aircraft.

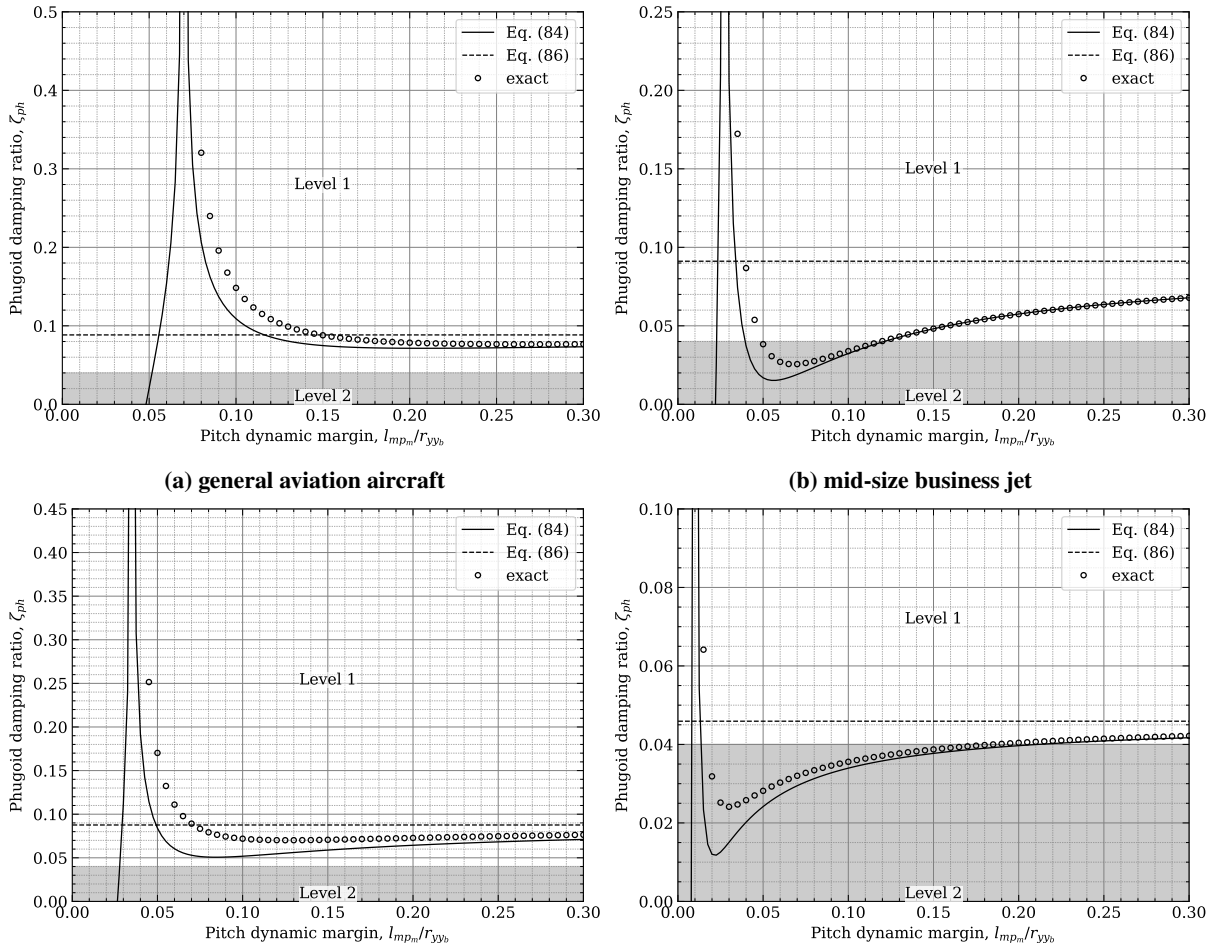

(a) general aviation aircraft

(b) mid-size business jet

(c) large commercial airliner

(d) fighter aircraft

Fig. 6 Change in phugoid mode handling qualities with dynamic margin.

As seen in Fig. 6, the damping ratio approximation in Eq. (84) follows the trend of the damping ratio found using a numerical eigenvalue analysis of the linearized aircraft system. As with the short-period mode, eigen analysis results are not reported below a given pitch dynamic margin because at these points the phugoid mode became non-oscillatory. While a lightly-damped oscillatory mode does reappear in the eigen analysis solution at smaller pitch dynamic margins, this mode seemed to be the pairing of 'former' short-period and phugoid mode eigenvalues. This phenomena warrants further study, but lies outside the scope of the present paper, and as such the values are not presented in Fig. 6.

The fighter aircraft has generally worse phugoid damping as the dynamic margin decreases. Indeed, both the fighter aircraft and mid-sized business jet have bounds on where the center of gravity cannot be located, due to the damping ratio dipping below level 1 handling qualities. The asymptotes depicted on each plot denote the passing of the center of gravity over the aircraft neutral point, and can be analytically determined by setting the term $\frac{m_{,\alpha}}{L_{,\alpha} r_{yy_b}}$ in Eq. (27) to zero. The presence of this asymptote suggests an aircraft may benefit from having the center of gravity located near the neutral point. This is obviously not the case for all aircraft, as these asymptotes for the mid-size business jet, larger commercial aircraft, and fighter aircraft in Fig. 6 are located outside level 1 short-period mode handling qualities as depicted in Fig. 5.

C. Roll Mode

The mode property generally used to measure the controllability of the roll mode is the time constant. The time constant can be determined (derived in the appendix, subsection A.C) as

$$\tau_{ro} = -\frac{I_{xx_b}}{\ell_{,p}} \tag{87}$$

There are thus two methods to decrease the roll mode transience: decrease the body-fixed moment of inertia about the x-axis, or increase the roll damping. The result given in Eq. (87) is similar to those presented in other developments [58, 66–68]. No further analysis will be dedicated to this mode due to negligible dependence on the roll static and dynamic margins defined in Eqs. (34) and (74), respectively. Note, an alternate roll dynamic margin dependent on roll damping may be useful in studying this mode (as well as the spiral mode, shown later) and warrants further study.

D. Spiral Mode

The mode property generally used to measure the controllability of the spiral mode is the time-to-double. The time-to-double can be determined (derived in the appendix, subsection A.D) as

$$\tau_{sl} = -\ln(2)\frac{1}{W}\frac{\frac{\ell_{,p}}{h_{np_\ell}} + \frac{n_{,p}}{l_{np_n}}}{\frac{h_{mp_\ell}}{h_{np_\ell}} - \frac{l_{mp_n}}{l_{np_n}}} \tag{88}$$

This spiral mode time-to-double approximation is similar to that in some formulations [45, 67]. Other formulations [58, 66, 68, 69] neglect the effects of the roll damping derivatives, as

$$\tau_{sl} = -\ln(2)\frac{1}{W}\frac{\frac{\frac{g}{V_O}I_{zz_b}}{l_{np_n}}}{\frac{h_{mp_\ell}}{h_{np_\ell}} - \frac{l_{mp_n}}{l_{np_n}}} \tag{89}$$

which has been noted as a particularly poor approximation [45, 66]. The formulation in Eq. (88) emphasizes the interplay between roll and yaw damping in the spiral mode. The interplay between the roll and yaw dynamic margins demonstrates the effect that, similar to the counter-intuitive phugoid characteristic, a slight shifting aft of the center of gravity may result in improved time to double of the spiral mode. This can be seen in Fig. 7 for typical representatives of four classes of aircraft.

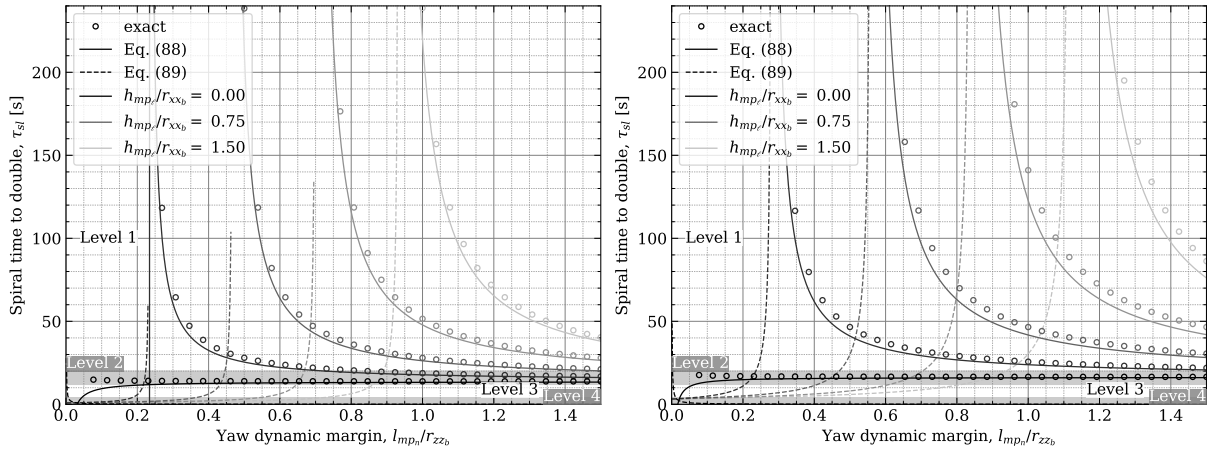

(a) general aviation aircraft

(b) mid-size business jet

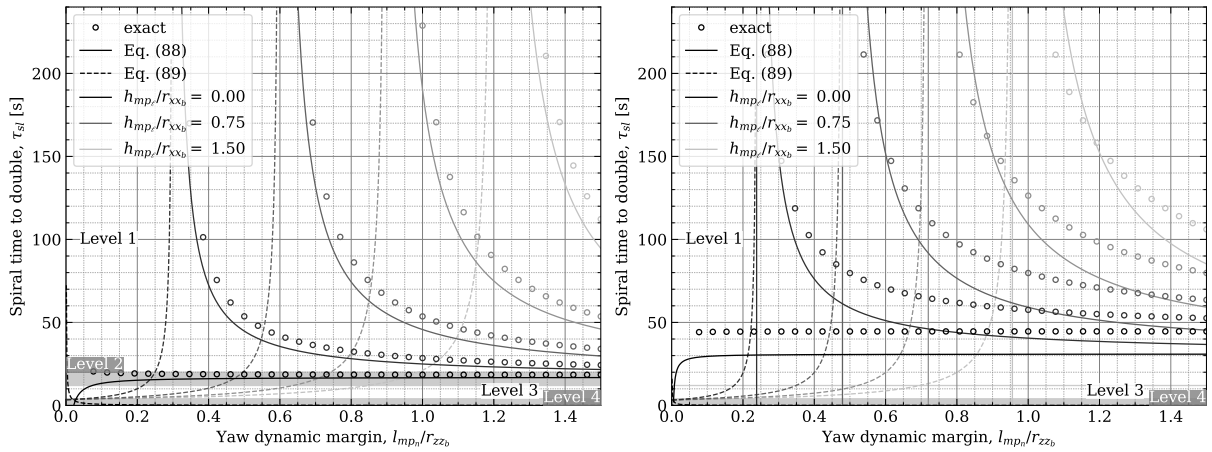

(c) large commercial airliner

(d) fighter aircraft

Fig. 7 Change in spiral mode handling qualities with roll and yaw dynamic margins.

As seen in Fig. 7, the time to double approximation in Eq. (88) follows the trend of the time to double found using a numerical eigenvalue analysis of the aircraft linearized system. Note, not only does Eq. (89) poorly predict the spiral mode time to double, it predicts a trend in which a shifting *forward* of the center of gravity will improve the time to double, unlike the trend predicted by Eq. (88) and manifested by the aircraft linearized system. These results validate the statement made by Cook regarding lateral maneuverability: "Remember that too much stability can be as hazardous as too little stability!" [51].

Figure 7 also shows the trend where if the roll dynamic margin is zero, the yaw dynamic margin has (near) zero effect on the spiral mode time to double. Generally with minimal roll dynamic margin ($\frac{h_{mp_\ell}}{r_{xx_b}} \lessapprox 0.375$) the spiral mode has level 1 handling qualities, and with increasing roll dynamic margin the spiral mode becomes stable at smaller yaw dynamic margins. The asymptotes on the plots in Fig. 7 indicate the spiral mode becoming stable (having a 'negative' doubling time) and thus having level 1 handling qualities with decreasing yaw dynamic margin. These asymptotes occur where the ratios of roll and yaw dynamic to static margin are equivalent (i.e. $\frac{h_{mp_\ell}}{h_{np_\ell}}$ and $\frac{l_{mp_n}}{l_{np_n}}$, respectively).

E. Dutch Roll Mode

The mode properties generally used to measure the controllability of the Dutch-roll mode are the damping rate, natural frequency, and damping ratio. The damping rate (derived in the appendix, subsection A.E) is

$$\sigma_{dr} = -\frac{1}{2}\left[\frac{Y_{,\beta}}{I_{zz_b}}\left(a_{zz_b} + I_{xx_b}\left(\frac{n_{,p}}{\ell_{,p}^2}h_{mp_\ell} - \frac{Wr_{zz_b}^2}{V_o\ell_{,p}^2}h_{np_\ell}\right) - \frac{\ell_{,r}n_{,p}}{Y_{,\beta}\ell_{,p}}\right) + \frac{W}{\ell_{,p}}\left(\frac{h_{mp_\ell}l_{np_n}}{l_{mp_n}} - h_{np_\ell}\right)\right] \tag{90}$$

where

$$a_{zz_b} = \frac{n_{,r}}{Y_{,\beta}} + \frac{r^2_{zz_b}}{V_o} \tag{91}$$

and the natural frequency (derived in the appendix, subsection A.E) is

$$\omega_{n_{dr}} = \left\{ \frac{1}{4} \left[\frac{Y_{,\beta}}{I_{zz_b}} \left(a_{zz_b} + I_{xx_b} \left(\frac{n_{,p}}{\ell^2_{,p}} h_{mp_\ell} - \frac{W r^2_{zz_b}}{V_o \ell^2_{,p}} h_{np_\ell} \right) - \frac{\ell_{,r} n_{,p}}{Y_{,\beta} \ell_{,p}} \right) + \frac{W}{\ell_{,p}} \left(\frac{h_{mp_\ell} l_{np_n}}{l_{mp_n}} - h_{np_\ell} \right) \right]^2 \right.$$
$$\left. - \frac{Y_{,\beta}}{I_{zz_b}} \left(l_{mp_n} + h_{mp_\ell} \frac{n_{,p}}{\ell_{,p}} - \frac{W r^2_{zz_b} h_{np_\ell}}{V_o \ell_{,p}} + \frac{1}{4} \frac{Y_{,\beta}}{I_{zz_b}} a^2_{zz_b} \right) \right\}^{1/2} \tag{92}$$

The damping ratio (derived in the appendix, subsection A.E) is thus

$$\zeta_{dr} = -\frac{1}{2} \left[\frac{Y_{,\beta}}{I_{zz_b}} \left(a_{zz_b} + I_{xx_b} \left(\frac{n_{,p}}{\ell^2_{,p}} h_{mp_\ell} - \frac{W r^2_{zz_b}}{V_o \ell^2_{,p}} h_{np_\ell} \right) - \frac{\ell_{,r} n_{,p}}{Y_{,\beta} \ell_{,p}} \right) + \frac{W}{\ell_{,p}} \left(\frac{h_{mp_\ell} l_{np_n}}{l_{mp_n}} - h_{np_\ell} \right) \right] \Bigg/$$
$$\left\{ \frac{1}{4} \left[\frac{Y_{,\beta}}{I_{zz_b}} \left(a_{zz_b} + I_{xx_b} \left(\frac{n_{,p}}{\ell^2_{,p}} h_{mp_\ell} - \frac{W r^2_{zz_b}}{V_o \ell^2_{,p}} h_{np_\ell} \right) - \frac{\ell_{,r} n_{,p}}{Y_{,\beta} \ell_{,p}} \right) + \frac{W}{\ell_{,p}} \left(\frac{h_{mp_\ell} l_{np_n}}{l_{mp_n}} - h_{np_\ell} \right) \right]^2 \right.$$
$$\left. - \frac{Y_{,\beta}}{I_{zz_b}} \left(l_{mp_n} + h_{mp_\ell} \frac{n_{,p}}{\ell_{,p}} - \frac{W r^2_{zz_b} h_{np_\ell}}{V_o \ell_{,p}} + \frac{1}{4} \frac{Y_{,\beta}}{I_{zz_b}} a^2_{zz_b} \right) \right\}^{1/2} \tag{93}$$

Neglecting coupling between roll, yaw, and sideslip angle results in mode property approximations similar to those in other developments [66–68, 70]:

$$\sigma_{dr} = -\frac{1}{2} \frac{Y_{,\beta}}{I_{zz_b}} a_{zz_b} \tag{94}$$

$$\omega_{n_{dr}} = \sqrt{-\frac{Y_{,\beta}}{I_{zz_b}} l_{mp_n}} \tag{95}$$

$$\zeta_{dr} = -\frac{1}{2} \sqrt{-\frac{Y_{,\beta}}{I_{zz_b} l_{mp_n}}} a_{zz_b} \tag{96}$$

These uncoupled solutions have been noted by Phillips [46], Nelson [66], Cook [67], and Schmidt [70] to give poor agreement with the true coupled Dutch-roll mode. The interplay between the roll and yaw dynamic margins can be seen in Figs. 8–10 for typical representatives of four classes of aircraft.

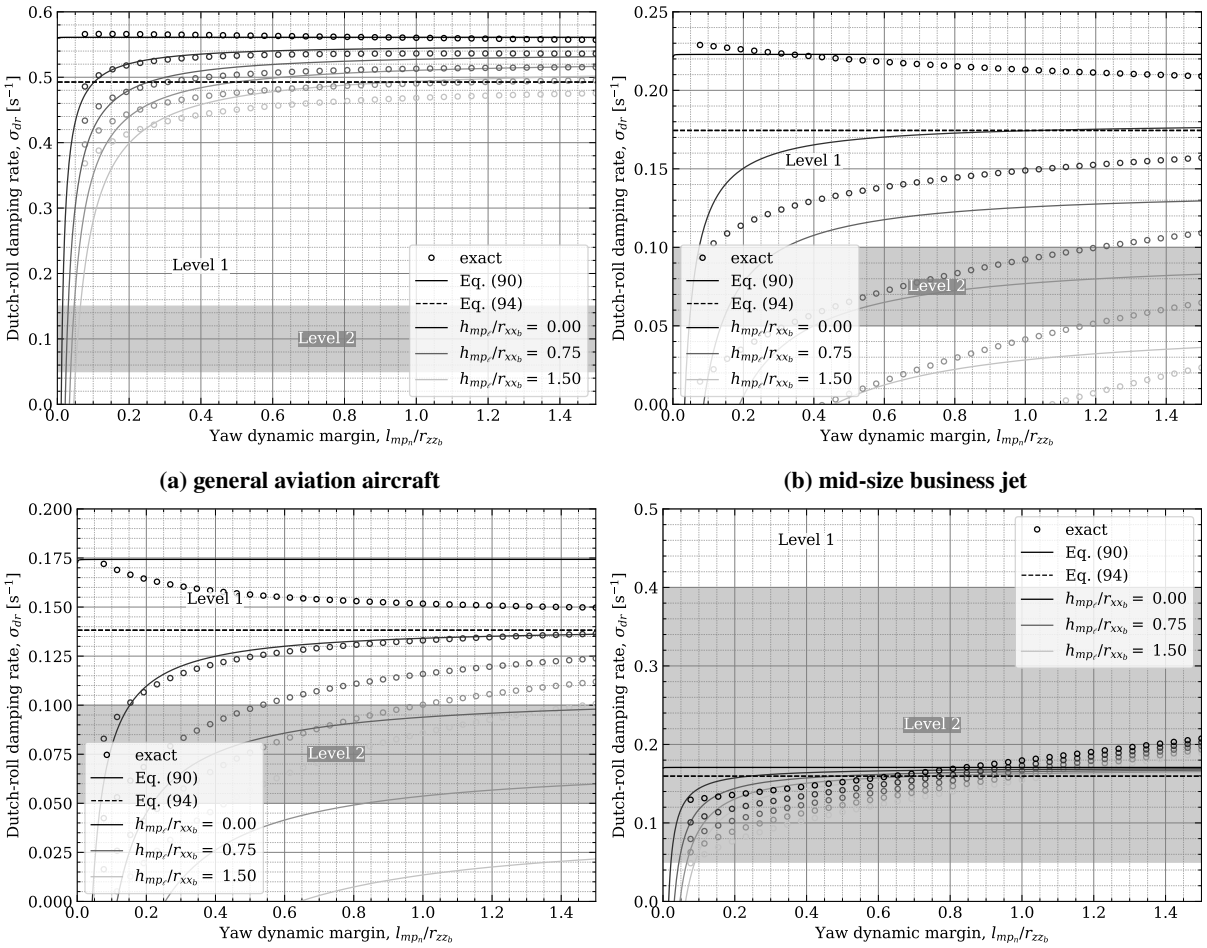

(a) general aviation aircraft

(b) mid-size business jet

(c) large commercial airliner

(d) fighter aircraft

Fig. 8 Change in Dutch-roll damping rate with roll and yaw dynamic margins.

Figure 8 shows the Dutch roll damping rate approximation in Eq. (90) to be accurate for some specific aircraft (general aviation aircraft, mid-size business jet) and poor for others. However the trends of the results are generally accurate. As will be shown later, this accuracy will have a minor effect when evaluating handling qualities. The trends shown in Fig. 8 predict the Dutch roll damping rate to improve with *increasing* yaw dynamic margin and *decreasing* roll dynamic margin. This demonstrates the effect previously noted by Phillips [46]: **increasing roll stability** will *decrease* Dutch roll damping and *increase* spiral damping, and **increasing yaw stability** will *increase* Dutch roll damping and *decrease* spiral damping. Note, however, the yaw dynamic margin has a minimal effect on the Dutch roll damping rate as yaw dynamic margin increases.

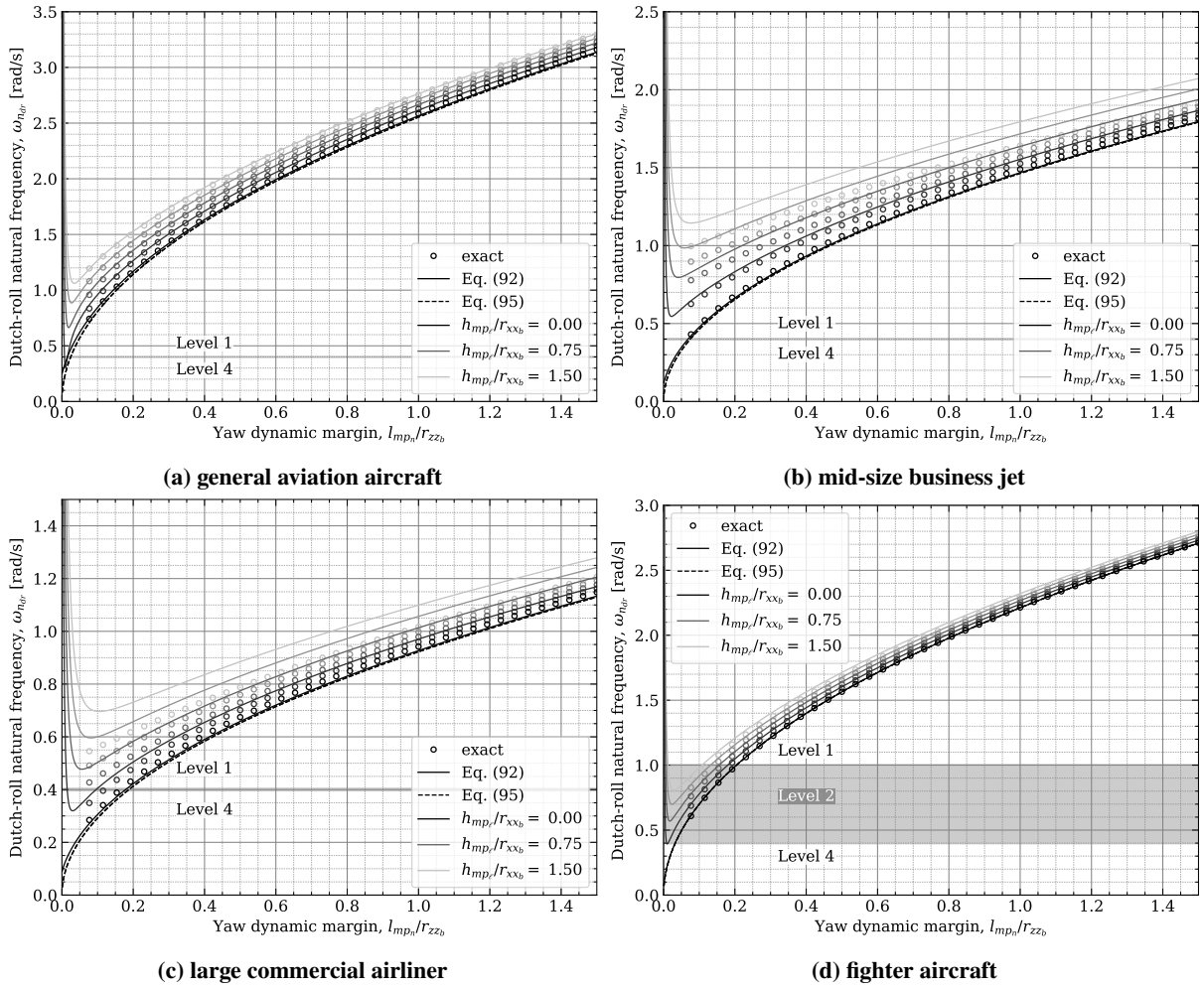

(a) general aviation aircraft

(b) mid-size business jet

(c) large commercial airliner

(d) fighter aircraft

Fig. 9 Change in Dutch-roll natural frequency with roll and yaw dynamic margins.

Figure 9 shows the Dutch roll natural frequency approximation in Eq. (92) to be accurate for the demonstrated aircraft. The trends of the results denote the Dutch roll natural frequency to increase with increasing yaw dynamic margin and / or roll dynamic margin. The Dutch roll natural frequency is less influenced by the roll dynamic margin than the yaw dynamic margin (particularly for certain aircraft: the general aviation aircraft and the fighter aircraft). This characteristic will be exploited later in the discussion of a Dutch roll analog to the short-period CAP.

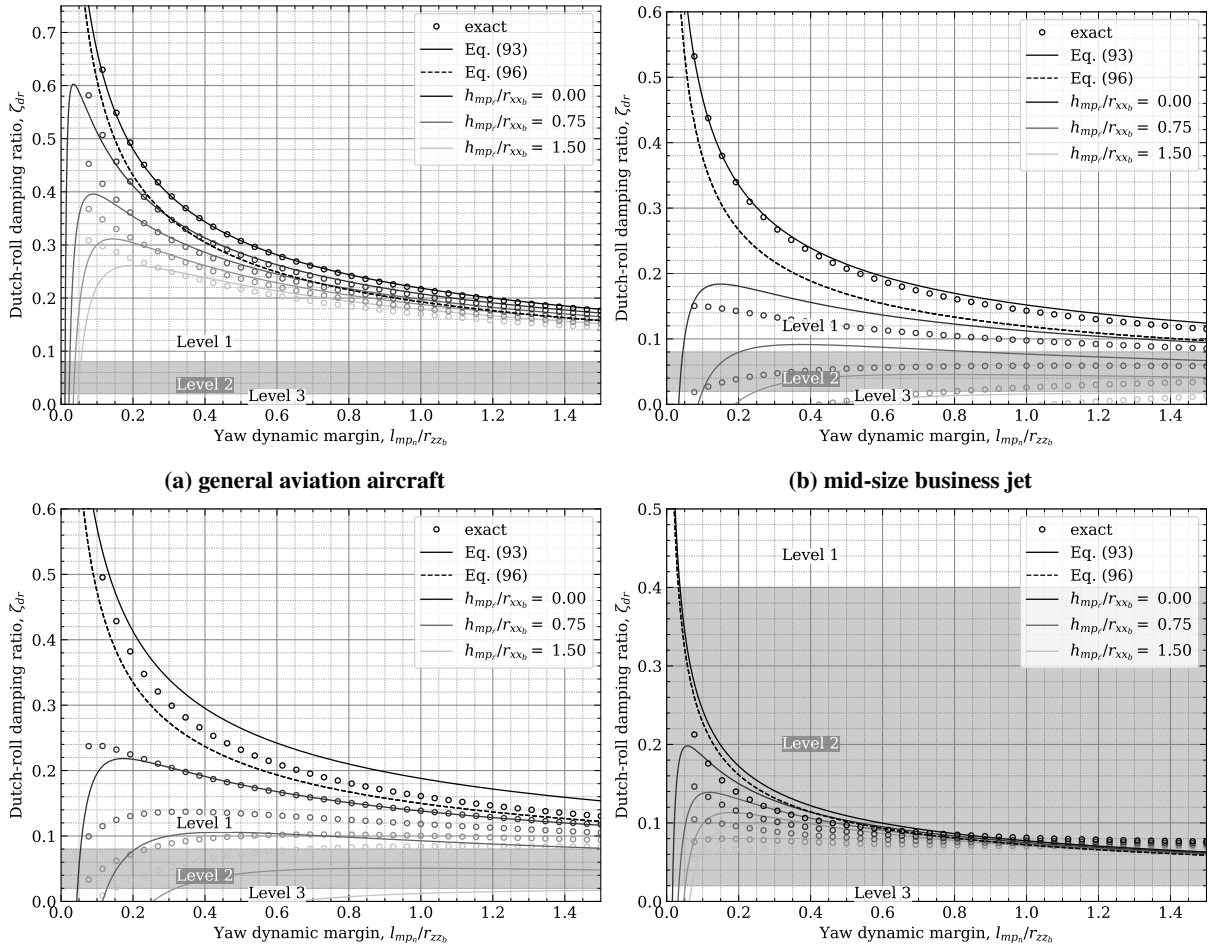

(a) general aviation aircraft

(b) mid-size business jet

(c) large commercial airliner

(d) fighter aircraft

Fig. 10 Change in Dutch-roll damping ratio with roll and yaw dynamic margins.

As seen in Fig. 10, the Dutch roll damping ratio approximation in Eq. (93) follows the trend of the Dutch roll damping ratio found using a numerical eigenvalue analysis of the aircraft linearized system. Note, Eq. (96) poorly predicts the Dutch-roll mode damping ratio as it does not account for the roll dynamic margin, unlike the trend predicted by Eq. (93). Figure 10 shows the trend of decreasing yaw dynamic margin and decreasing roll dynamic margin results in improved Dutch-roll damping ratio generally.

As seen in Fig. 10 while the Dutch roll damping ratio does depend significantly on the roll dynamic margin, recall the Dutch roll natural frequency shown in Fig. 9 is not as strongly dependant on the roll dynamic margin. Neglecting the effect of roll dynamic margin and roll static margin on the Dutch roll natural frequency results in the same approximation used in other formulations, given in Eq. (95). The formulation of the approximate Dutch roll natural frequency in Eq. (95) was determined assuming no coupling between roll, yaw, and sideslip. With these assumptions in mind, the authors note the similarity between the flawed Dutch-roll in Eq. (92) and short-period approximated natural frequency given in Eq. (A.7). An alternate version of the CAP defined by Bihrle [48] and studied by Phillips and Niewoehner [40, 59] as shown in Eq. (78) could be developed for the Dutch roll oscillation as

$$\mathrm{CAP}_{dr} = -\frac{\omega_{n_{dr}}^2}{\partial n_S/\partial\beta} \approx -\frac{\omega_{n_{dr}}^2}{C_{S,\beta}/C_W} = \frac{g l_{mp_n}}{r_{zz_b}^2} \tag{97}$$

The Dutch roll natural frequency has been noted as heavily dependent on the yaw static stability, yaw damping, and yaw inertia [46, 71], which are the principal components of the yaw dynamic margin. Also, the side acceleration has frequently been used in feedback for aircraft yaw dampers, which are used to improve Dutch roll oscillations [72, 73].

These reasons support the development of a Dutch roll CAP to evaluate the Dutch roll handling qualities of an aircraft. Similar to the pitch angular acceleration, the requirement for the yaw dynamic margin can be defined by rearranging Eq. (97) in terms of a yaw angular acceleration limit $\dot{r}_c$, as

$$\frac{l_{mp_n}}{r_{zz_b}} \geq \frac{\dot{r}_c}{g/r_{zz_b}} \tag{98}$$

The handling qualities of the Dutch roll mode can be seen in Fig. 11 as a function of yaw and roll dynamic margins. In Fig. 11 the Dutch roll damping ratio was determined from Eq. (93) and the Dutch roll CAP from Eq. (97). The handling quality limits for the Dutch roll CAP were determined for each aircraft from those set on the Dutch roll natural frequency.

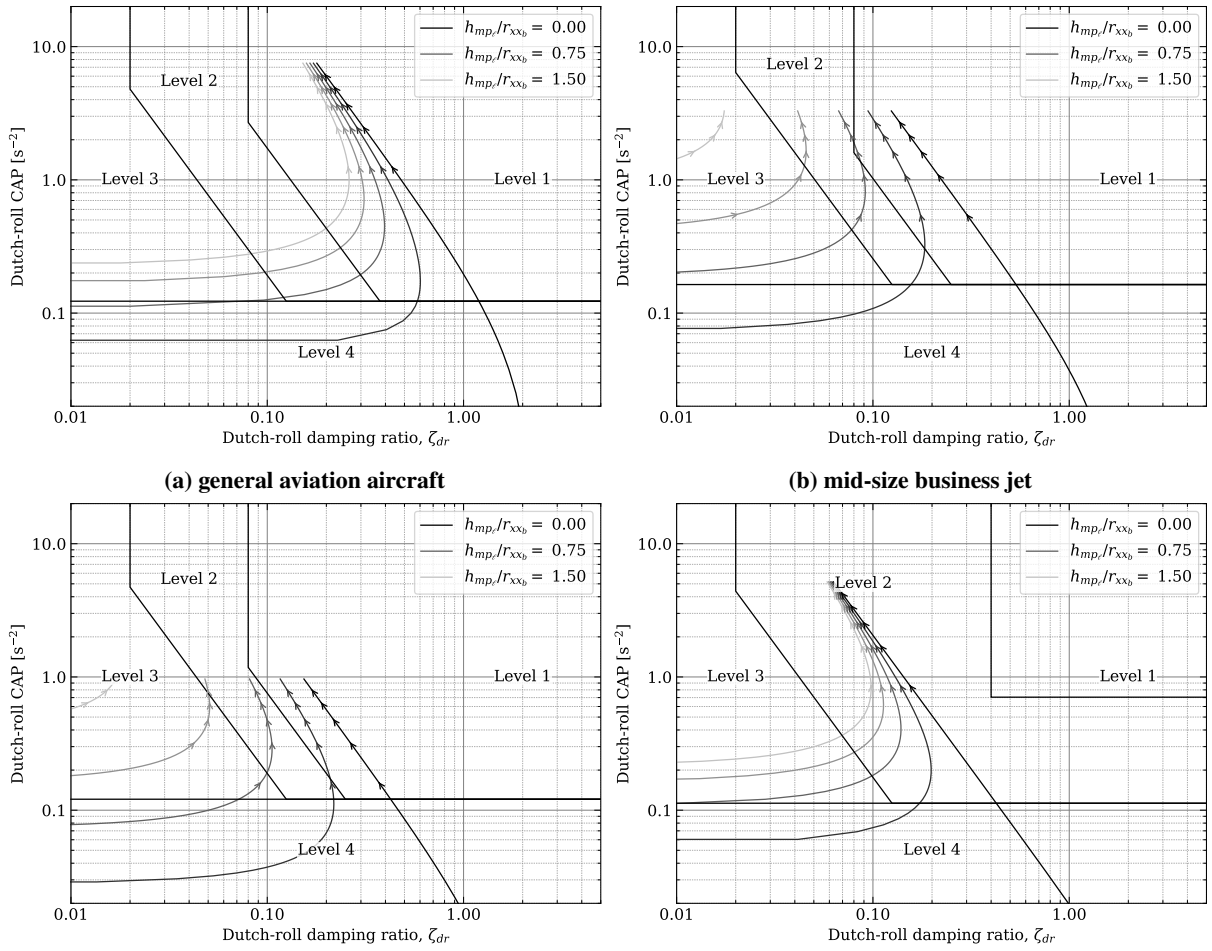

(a) general aviation aircraft

(b) mid-size business jet

(c) large commercial airliner

(d) fighter aircraft

Fig. 11 Change in Dutch-roll CAP with yaw dynamic margin, arrows indicating the direction of increasing yaw dynamic margin in increments of 25%.

The trends shown in Fig. 11 denote the Dutch roll handling quality to generally worsen with increasing yaw dynamic margin and increasing roll dynamic margin. The calculated Dutch roll CAP in Eq. (97) does not depend on the roll dynamic margin, which can be seen in the arrow heads which are located at the same CAP values regardless of roll dynamic margin.

Large transport aircraft typically require yaw dampers to mitigate Dutch roll oscillation and an example of this poor Dutch roll oscillatory behavior is readily seen for the large commercial airliner in Fig. 11. Particularly noteworthy is the effect increasing yaw dynamic margin has on the Dutch roll handling qualities where the roll dynamic margin is zero.

This response (increasing CAP, decreasing damping ratio) is very similar to that of the short-period handling qualities change with increasing pitch dynamic margin shown in Fig. 5 (increasing CAP, decreasing damping ratio).

One large difference is noticeable between the short-period and Dutch roll handling qualities regions: there are no upper limits placed on the Dutch roll CAP. It has been noted that the human brain is more susceptible to damage during rotational acceleration in increasing order to accelerations in: pitch, yaw, and roll [74]. Because the lower limits on the short-period CAP in Fig. 5 are similar to those on the Dutch roll CAP in Fig. 11 one may expect there to be upper limits on the Dutch roll CAP as there are limits on the short-period CAP, and the brain is more sensitive to yaw accelerations than pitch. Note, the side-force load factor derivative $\frac{\partial n_S}{\partial \beta} \approx \frac{C_{Y,\beta}}{C_W}$ is generally an order of magnitude smaller than the normal load factor derivative $\frac{\partial n_N}{\partial \alpha} \approx \frac{C_{L,\alpha}}{C_W}$ for a typical aircraft. This means the Dutch roll natural frequency for a given CAP limit is generally smaller than the short-period natural frequency. If the brain is more sensitive to yaw acceleration, and assuming the upper short-period CAP limit to apply to the Dutch roll oscillations, why is there no upper limit on the Dutch roll frequency? The frequencies for the Dutch roll mode are generally smaller than those encountered with the short-period mode. As the lift force is the greatest in magnitude on the aircraft, the effect of lift-induced oscillations (i.e. pitch) will be greater in magnitude (and thus sensitivity) than those induced by the side-force (i.e. yaw).

Further comparison between modes may be misleading because the handling qualities for a given mode assume level 1 handling qualities for all other modes. Further work should study the proposed Dutch roll CAP and whether upper limits may be (or whether the plotted lower limits are) appropriate for the Dutch roll CAP.

V. Conclusions

The pitch neutral point and associated static margin have long been recognized as a measure of longitudinal static stability. More recently, a pitch dynamic margin was proposed, and the direct relationship to short-period handling qualities and limits on the dynamic margin were presented. The present work extends these concepts to consider the existence of roll and yaw neutral points and associated static margins, and roll and yaw maneuver points and associated dynamic margins, which can be related to lateral handling quality limits.

The aircraft handling qualities are a fundamental measure of the uncontrolled damping response to disturbance. The handling qualities of aircraft have been studied extensively, and approximations for calculating them have been developed. These approximations can have varying levels of accuracy based on the assumptions used. The approximations presented in the present paper are based on those of Phillips [42–46].

The derivations for the pitch static margin [39] and longitudinal dynamic margin [40, 41] given by Phillips and Niewoehner were replicated for completeness. Dimensionless dynamic rates were then derived for pitch and yaw based on the aircraft body-fixed acceleration equations of motion. Static margins were then derived for roll and yaw in Eqs. (34) and (39), respectively. The dynamic yaw rate relation to side-force load factor was used to derive roll and yaw dynamic margins in Eqs. (74) and (75).

The dynamic mode approximations developed by Phillips [42–46] and alternately presented by Hunsaker et al. [47] were rearranged in Eqs. (78)–(97) to emphasize the effects of roll, pitch, and yaw static and dynamic margins on the aircraft handling-qualities. Particular emphasis was placed on the phugoid, spiral, and Dutch-roll modes. A Dutch-roll analog to the short-period CAP was developed and analyzed. This Dutch roll CAP is proposed for use in evaluating the oscillatory nature of the Dutch roll mode on aircraft, and depends significantly on the yaw dynamic margin.

The relationships evident in the presented dynamic mode approximations provide general principles for the early phases of the aircraft design process. While past studies have noted the correlation between pitch dynamic margin and longitudinal handling qualities, the present method correlates the relationships between the roll, pitch and yaw static and dynamic margins and longitudinal and lateral handling qualities. This was done to improve understanding of how these parameters affect the handling qualities of an aircraft, such as the motivation for shifting the aircraft cg aft for improved handling characteristics. These types of relationships can have a significant impact on the aircraft design process, and are not obvious in other formulations. The presented dynamic mode approximations can be used with handling quality limits to establish acceptable center of gravity locations on a given aircraft to maintain level 1 handling qualities.

A. Appendix

This appendix includes detailed derivations for the closed-form mode approximations, which are included in the main body of this paper. While these derivations are performed using the equations and coefficients presented by Hunsaker et. al. [47], these derivations could as easily be performed using the equations and coefficients developed by Phillips [42–46].

A. Short-Period Mode

The damping rate can be determined from the closed-form equation for σ_{sp} as [47]

$$\sigma_{sp} = -\frac{1}{2}\frac{g}{V_o}\left(K_{z,\alpha} + K_{m,\breve{q}} + K_{m,\hat{\alpha}}\right) \tag{A.1}$$

the terms can be redimensionalized as

$$\sigma_{sp} = -\frac{1}{2}\frac{g}{V_o}\left(\frac{-D_o - L_{,\alpha}}{W} + \frac{V_o m_{,q}}{g I_{yy_b}} + \frac{V_o m_{,\dot{\alpha}}}{g I_{yy_b}}\right) \tag{A.2}$$

and simplify (note, $L_{,a}$ is typically 2 orders of magnitude larger than D_o), as

$$\sigma_{sp} = -\frac{1}{2}\frac{1}{I_{yy_b} L_{,\alpha}}\left(\frac{m_{,\dot{\alpha}}}{L_{,\alpha}} + a_{yy_b}\right) \tag{A.3}$$

where

$$a_{yy_b} = \frac{m_{,q}}{L_{,\alpha}} - \frac{r_{yy_b}^2}{V_o}$$

The damped natural frequency is determined from the closed-form equation as [47]

$$\omega_{d_{sp}} = \frac{g}{V_o}\sqrt{\left(K_{z,\alpha} K_{m,\breve{q}} - K_{m,\alpha}\right) - \left(\frac{K_{z,\alpha} + K_{m,\breve{q}} + K_{m,\hat{\alpha}}}{2}\right)^2} \tag{A.4}$$

the terms can be redimensionalized as

$$\omega_{d_{sp}} = \frac{g}{V_o}\sqrt{\left(\frac{-D_o - L_{,\alpha}}{W}\frac{V_o m_{,q}}{g I_{yy_b}} - \frac{V_o^2 m_{,\alpha}}{g^2 I_{yy_b}}\right) - \frac{1}{4}\left(\frac{-D_o - L_{,\alpha}}{W} + \frac{V_o m_{,q}}{g I_{yy_b}} + \frac{V_o m_{,\dot{\alpha}}}{g I_{yy_b}}\right)^2} \tag{A.5}$$

and simplify (note, $L_{,a}$ is typically 2 orders of magnitude larger than D_o), as

$$\omega_{d_{sp}} = \sqrt{g\frac{L_{,\alpha}}{W}\frac{l_{mp_m}}{r_{yy_b}^2} - \frac{1}{4}\frac{1}{I_{yy_b}^2 L_{,\alpha}^2}\left(\frac{m_{,\dot{\alpha}}}{L_{,\alpha}} + a_{yy_b}\right)^2} \tag{A.6}$$

The natural frequency is determined from the closed-form equation as [47]

$$\omega_{n_{sp}} = \sqrt{\sigma_{sp}^2 + \omega_{d_{sp}}^2} = \frac{g}{V_o}\sqrt{K_{z,\alpha} K_{m,\breve{q}} - K_{m,\alpha}} = \frac{\sqrt{g\frac{L_{,\alpha}}{W} l_{mp_m}}}{r_{yy_b}} \tag{A.7}$$

The short-period damping ratio thus becomes

$$\zeta_{sp} = \frac{\sigma_{sp}}{\omega_{n_{sp}}} = -\frac{1}{2}\sqrt{\frac{L_{,\alpha}}{I_{yy_b} l_{mp_m}}}\left(\frac{m_{,\dot{\alpha}}}{L_{,\alpha}} + a_{yy_b}\right) \tag{A.8}$$

B. Phugoid Mode

The damping rate can be determined from the closed-form equation for σ_{ph} as [47]

$$\sigma_{ph} = -\frac{g}{V_o}\left[-\frac{K_{z,\mu}}{2}\left(-\frac{K_{x,\mu}}{K_{z,\mu}} + R_{Pd} - R_{Pp}\right)\right] \tag{A.9}$$

the ratios derived for the phugoid mode are inserted as

$$\sigma_{ph} = \frac{g}{V_o}\frac{K_{z,\mu}}{2}\left[-\frac{K_{x,\mu}}{K_{z,\mu}} + \frac{K_{x,\alpha} K_{m,\breve{q}}}{K_{m,\alpha} - K_{z,\alpha} K_{m,\breve{q}}} - \frac{K_{m,\alpha}(K_{z,\alpha} + K_{m,\breve{q}})}{(K_{m,\alpha} - K_{z,\alpha} K_{m,\breve{q}})^2}\right] \tag{A.10}$$

Several terms can be dropped due to their relative importance (2 orders of magnitude), particularly terms which are multiplied values.

$$\sigma_{ph} = \frac{g}{V_o}\frac{K_{z,\mu}}{2}\left[-\frac{K_{x,\mu}}{K_{z,\mu}} - \frac{K_{m,\alpha}(K_{z,\alpha} + K_{m,\check{q}})}{(K_{m,\alpha} - K_{z,\alpha}K_{m,\check{q}})^2}\right] \tag{A.11}$$

the terms are redimensionalized as

$$\sigma_{ph} = \frac{g}{V_o}\frac{L_o}{W}\left[\frac{-2\frac{D_o}{W}}{2\frac{L_o}{W}} - \frac{\frac{V_o^2 m_{,\alpha}}{g^2 I_{yy_b}}\left(\frac{-D_o - L_{,\alpha}}{W} + \frac{V_o m_{,q}}{g I_{yy_b}}\right)}{\left(\frac{V_o^2 m_{,\alpha}}{g^2 I_{yy_b}} - \frac{-D_o - L_{,\alpha}}{W}\frac{V_o m_{,q}}{g I_{yy_b}}\right)^2}\right] \tag{A.12}$$

and simplified (note, typically $L_{,a} >> D_o$), as

$$\sigma_{ph} = \frac{g}{V_o}\left[\frac{D_o}{W} + \frac{g}{V_o}\frac{L_o}{W}\frac{l_{np_m}}{l_{mp_m}^2}a_{yy_b}\right] \tag{A.13}$$

The closed form approximation of the phugoid mode natural frequency is [47]

$$\omega_{n_{ph}} = \frac{g}{V_o}\frac{K_{z,\mu}}{2}\sqrt{\left(-\frac{K_{x,\mu}}{K_{z,\mu}} + R_{Pd} - R_{Pp}\right)^2 + \frac{4}{K_{z,\mu}}R_{Ps} - \left(\frac{K_{x,\mu}}{-K_{z,\mu} + R_{Pd}}\right)^2} \tag{A.14}$$

the ratios derived for the phugoid mode are inserted as

$$\omega_{n_{ph}} = \frac{g}{V_o}\frac{K_{z,\mu}}{2}\left[\left(-\frac{K_{x,\mu}}{K_{z,\mu}} + \frac{K_{x,\alpha}K_{m,\check{q}}}{K_{m,\alpha} - K_{z,\alpha}K_{m,\check{q}}} - \frac{K_{m,\alpha}(K_{z,\alpha} + K_{m,\check{q}})}{(K_{m,\alpha} - K_{z,\alpha}K_{m,\check{q}})^2}\right)^2 \tag{A.15}$$

$$+ \frac{4}{K_{z,\mu}}\frac{K_{m,\alpha}}{K_{m,\alpha} - K_{z,\alpha}K_{m,\check{q}}} - \left(\frac{K_{x,\mu}}{-K_{z,\mu} + \frac{K_{x,\alpha}K_{m,\check{q}}}{K_{m,\alpha} - K_{z,\alpha}K_{m,\check{q}}}}\right)^2\Bigg]^{1/2} \tag{A.16}$$

Several terms can be dropped due to their relative importance (2 orders of magnitude), particularly terms which are multiplied values.

$$\omega_{n_{ph}} = \frac{g}{V_o}\sqrt{\frac{K_{z,\mu}K_{m,\alpha}}{K_{m,\alpha} - K_{z,\alpha}K_{m,\check{q}}}} \tag{A.17}$$

the terms are redimensionalized as

$$\omega_{n_{ph}} = \frac{g}{V_o}\sqrt{\frac{2\frac{L_o}{W}\frac{V_o^2 m_{,\alpha}}{g^2 I_{yy_b}}}{\frac{V_o^2 m_{,\alpha}}{g^2 I_{yy_b}} - \frac{-D_o - L_{,\alpha}}{W}\frac{V_o m_{,q}}{g I_{yy_b}}}} \tag{A.18}$$

and simplify (note, $L_{,a}$ is typically 2 orders of magnitude larger than D_o), as

$$\omega_{n_{ph}} = \frac{g}{V_o}\sqrt{\frac{2L_o m_{,\alpha}}{W m_{,\alpha} + \frac{g}{V_o}L_{,\alpha}m_{,q}}} = \frac{g}{V_o}\sqrt{\frac{2L_o m_{,\alpha}}{-W L_{,\alpha}\left(-\frac{m_{,\alpha}}{L_{,\alpha}} - \frac{m_{,q}}{W}\frac{g}{V_o}\right)}} = \frac{g}{V_o}\sqrt{\frac{2L_o l_{np_m}}{W l_{mp_m}}} \tag{A.19}$$

The phugoid damping ratio thus becomes

$$\zeta_{ph} = \frac{\sigma_{ph}}{\omega_{n_{ph}}} = \frac{D_o}{W}\sqrt{\frac{W l_{mp_m}}{2L_o l_{np_m}}} + \frac{g}{V_o}\sqrt{\frac{L_o l_{np_m}}{2W l_{mp_m}^3}}a_{yy_b} \tag{A.20}$$

C. Roll

The roll mode time constant is found as [47]

$$\tau_{ro} = -\frac{1}{\sigma_{ro}} = -\frac{V_o}{g}\frac{1}{K_{\ell,\check{p}}} = -\frac{V_o}{g}\frac{1}{\frac{V_o \ell_{,p}}{g I_{xx_b}}} = -\frac{I_{xx_b}}{\ell_{,p}} \tag{A.21}$$

D. Spiral Mode

The spiral mode time to double is found as [47]

$$\tau_{sl} = -\frac{\ln(2)}{\sigma_{sl}} = -\ln(2)\frac{V_o}{g}\frac{K_{\ell,\beta}K_{n,\check{p}} - K_{\ell,\check{p}}K_{n,\beta}}{K_{\ell,\beta}K_{n,\check{r}} - K_{\ell,\check{r}}K_{n,\beta}} \tag{A.22}$$

The K values are redimensionalized as

$$\tau_{sl} = -\ln(2)\frac{V_o}{g}\frac{\frac{V_o^2\ell_{,\beta}}{g^2I_{xx_b}}\frac{V_o n_{,p}}{gI_{zz_b}} - \frac{V_o\ell_{,p}}{gI_{xx_b}}\frac{V_o^2 n_{,\beta}}{g^2I_{zz_b}}}{\frac{V_o^2\ell_{,\beta}}{g^2I_{xx_b}}\frac{V_o n_{,r}}{gI_{zz_b}} - \frac{V_o\ell_{,r}}{gI_{xx_b}}\frac{V_o^2 n_{,\beta}}{g^2I_{zz_b}}} \tag{A.23}$$

Which simplifies to

$$\tau_{sl} = -\ln(2)\frac{V_o}{g}\frac{\ell_{,\beta}n_{,p} - \ell_{,p}n_{,\beta}}{\ell_{,\beta}n_{,r} - \ell_{,r}n_{,\beta}} \tag{A.24}$$

In which the side-force slope can be inserted as

$$\tau_{sl} = -\ln(2)\frac{V_o}{g}\frac{\frac{\ell_{,\beta}}{Y_{,\beta}}n_{,p} - \ell_{,p}\frac{n_{,\beta}}{Y_{,\beta}}}{\frac{\ell_{,\beta}}{Y_{,\beta}}n_{,r} - \ell_{,r}\frac{n_{,\beta}}{Y_{,\beta}}} \tag{A.25}$$

the roll and yaw static margins can be inserted as

$$\tau_{sl} = -\ln(2)\frac{V_o}{g}\frac{h_{np_\ell}n_{,p} + \ell_{,p}l_{np_n}}{h_{np_\ell}n_{,r} + \ell_{,r}l_{np_n}} \tag{A.26}$$

and rearranged as

$$\tau_{sl} = -\ln(2)\frac{\frac{n_{,p}}{l_{np_n}} + \frac{\ell_{,p}}{h_{np_\ell}}}{\frac{n_{,r}\frac{g}{V}}{l_{np_n}} + \frac{\ell_{,r}\frac{g}{V}}{h_{np_\ell}}} \tag{A.27}$$

The components of the roll and yaw dynamic margins in Eqs. (72) and (73) can be rearranged to give

$$W\left(\frac{h_{mp_\ell}}{h_{np_\ell}} - 1\right) = \frac{\ell_{,r}\frac{g}{V}}{h_{np_\ell}} \tag{A.28}$$

$$W\left(1 - \frac{l_{mp_n}}{l_{np_n}}\right) = \frac{n_{,r}\frac{g}{V}}{l_{np_n}} \tag{A.29}$$

and the components of the roll and yaw dynamic margins can be inserted as

$$\tau_{sl} = -\ln(2)\frac{1}{W}\frac{\frac{\ell_{,p}}{h_{np_\ell}} + \frac{n_{,p}}{l_{np_n}}}{\frac{h_{mp_\ell}}{h_{np_\ell}} - \frac{l_{mp_n}}{l_{np_n}}} \tag{A.30}$$

E. Dutch Roll Mode

First the Dutch-roll damping rate is calculated as [47]

$$\sigma_{dr} = -\frac{1}{2}\frac{g}{V_o}\left(K_{y,\beta} + K_{n,\check{r}} - R_{Dc} + R_{Dp}\right) \tag{A.31}$$

the ratios can be inserted as

$$\sigma_{dr} = -\frac{1}{2}\frac{g}{V_o}\left(K_{y,\beta} + K_{n,\check{r}} - \frac{K_{\ell,\check{r}}K_{n,\check{p}}}{K_{\ell,\check{p}}} + \frac{K_{\ell,\check{r}}K_{n,\beta} - K_{\ell,\beta}K_{n,\check{r}}}{K_{\ell,\check{p}}\left(K_{n,\beta} + K_{y,\beta}K_{n,\check{r}}\right)} - \frac{K_{\ell,\beta}\left[1 - \left(1 - K_{y,\check{r}}\right)K_{n,\check{p}}\right] - K_{y,\beta}K_{\ell,\check{r}}K_{n,\check{p}}}{K_{\ell,\check{p}}^2}\right) \tag{A.32}$$

Typically $1 >> K_{y,\check{r}}$,

$$\sigma_{dr} = -\frac{1}{2}\frac{g}{V_o}\left(K_{y,\beta} + K_{n,\check{r}} - \frac{K_{\ell,\check{r}}K_{n,\check{p}}}{K_{\ell,\check{p}}} + \frac{1}{K_{\ell,\check{p}}}\frac{K_{\ell,\check{r}}K_{n,\beta} - K_{\ell,\beta}K_{n,\check{r}}}{K_{n,\beta} + K_{y,\beta}K_{n,\check{r}}} - \frac{K_{\ell,\beta}}{K_{\ell,\check{p}}^2} + \left(K_{\ell,\beta} + K_{y,\beta}K_{\ell,\check{r}}\right)\frac{K_{n,\check{p}}}{K_{\ell,\check{p}}^2}\right) \tag{A.33}$$

The following terms can be redimensionalized and simplified as

$$\begin{array}{c|c|c|c}
K_{n,\beta} + K_{y,\beta}K_{n,\check{r}} & K_{\ell,\beta} + K_{y,\beta}K_{\ell,\check{r}} & K_{\ell,\check{r}}K_{n,\beta} - K_{\ell,\beta}K_{n,\check{r}} & K_{y,\beta} + K_{n,\check{r}} \\
\frac{V_o^2 n_{,\beta}}{g^2 I_{zz_b}} + \frac{Y_{,\beta}}{W}\frac{V_o n_{,r}}{g I_{zz_b}} & \frac{V_o^2 \ell_{,\beta}}{g^2 I_{xx_b}} + \frac{Y_{,\beta}}{W}\frac{V_o \ell_{,r}}{g I_{xx_b}} & \frac{V_o \ell_{,r}}{g I_{xx_b}}\frac{V_o^2 n_{,\beta}}{g^2 I_{zz_b}} - \frac{V_o^2 \ell_{,\beta}}{g^2 I_{xx_b}}\frac{V_o n_{,r}}{g I_{zz_b}} & \frac{Y_{,\beta}}{W} + \frac{V_o n_{,r}}{g I_{zz_b}} \\
-\frac{V_o^2}{g^2}\frac{Y_{,\beta}}{I_{zz_b}}\left(-\frac{n_{,\beta}}{Y_{,\beta}} - \frac{n_{,r}\frac{g}{V_o}}{W}\right) & \frac{V_o^2}{g^2}\frac{Y_{,\beta}}{I_{xx_b}}\left(\frac{\ell_{,\beta}}{Y_{,\beta}} + \frac{\ell_{,r}\frac{g}{V_o}}{W}\right) & -\frac{V_o^3}{g^3}\frac{Y_{,\beta}}{I_{xx_b}I_{zz_b}}\left(h_{np_\ell}n_{,r} + \ell_{,r}l_{np_n}\right) & \frac{V_o Y_{,\beta}}{g I_{zz_b}}\left(\frac{n_{,r}}{Y_{,\beta}} + \frac{r_{zz_b}^2}{V_o}\right) \\
-\frac{V_o^2}{g^2}\frac{Y_{,\beta}}{I_{zz_b}}l_{mp_n} & \frac{V_o^2}{g^2}\frac{Y_{,\beta}}{I_{xx_b}}h_{mp_\ell} & -\frac{V_o^4}{g^4}\frac{Y_{,\beta}W}{I_{xx_b}I_{zz_b}}\left(h_{mp_\ell}l_{np_n} - l_{mp_n}h_{np_\ell}\right) & \frac{V_o Y_{,\beta}}{g I_{zz_b}}a_{zz_b}
\end{array}$$

the terms are redimensionalized as

$$\sigma_{dr} = -\frac{1}{2}\frac{g}{V_o}\left(\frac{V_o Y_{,\beta}}{g I_{zz_b}}a_{zz_b} - \frac{\frac{V_o \ell_{,r}}{g I_{xx_b}}\frac{V_o n_{,p}}{g I_{zz_b}}}{\frac{V_o \ell_{,p}}{g I_{xx_b}}} + \frac{1}{\frac{V_o \ell_{,p}}{g I_{xx_b}}}\frac{-\frac{V_o^4}{g^4}\frac{Y_{,\beta}W}{I_{xx_b}I_{zz_b}}\left(h_{mp_\ell}l_{np_n} - l_{mp_n}h_{np_\ell}\right)}{-\frac{V_o^2}{g^2}\frac{Y_{,\beta}}{I_{zz_b}}l_{mp_n}} - \frac{\frac{V_o^2 \ell_{,\beta}}{g^2 I_{xx_b}}}{\left(\frac{V_o \ell_{,p}}{g I_{xx_b}}\right)^2} + \frac{V_o^2}{g^2}\frac{Y_{,\beta}}{I_{xx_b}}h_{mp_\ell}\frac{\frac{V_o n_{,p}}{g I_{zz_b}}}{\left(\frac{V_o \ell_{,p}}{g I_{xx_b}}\right)^2}\right) \tag{A.34}$$

and simplified, as

$$\sigma_{dr} = -\frac{1}{2}\left[\frac{Y_{,\beta}}{I_{zz_b}}\left(a_{zz_b} + I_{xx_b}\left(\frac{n_{,p}}{\ell_{,p}^2}h_{mp_\ell} - \frac{W r_{zz_b}^2}{V_o \ell_{,p}^2}h_{np_\ell}\right) - \frac{\ell_{,r}n_{,p}}{Y_{,\beta}\ell_{,p}}\right) + \frac{W}{\ell_{,p}}\left(\frac{h_{mp_\ell}l_{np_n}}{l_{mp_n}} - h_{np_\ell}\right)\right] \tag{A.35}$$

where

$$a_{zz_b} = \frac{n_{,r}}{Y_{,\beta}} + \frac{r_{zz_b}^2}{V_o}$$

The Dutch-roll damped natural frequency is calculated as [47]

$$\omega_{d_{dr}} = \frac{g}{V_o}\sqrt{\left(1 - K_{y,\check{r}}\right)K_{n,\beta} + K_{y,\beta}K_{n,\check{r}} + R_{Ds} - \left(\frac{K_{y,\beta} + K_{n,\check{r}}}{2}\right)^2} \tag{A.36}$$

the R_{Ds} ratio can be inserted as

$$\omega_{d_{dr}} = \frac{g}{V_o}\sqrt{\left(1 - K_{y,\check{r}}\right)K_{n,\beta} + K_{y,\beta}K_{n,\check{r}} + \frac{K_{\ell,\beta}\left[1 - \left(1 - K_{y,\check{r}}\right)K_{n,\check{p}}\right] - K_{y,\beta}K_{\ell,\check{r}}K_{n,\check{p}}}{K_{\ell,\check{p}}} - \left(\frac{K_{y,\beta} + K_{n,\check{r}}}{2}\right)^2} \tag{A.37}$$

Typically $1 >> K_{y,\check{r}}$,

$$\omega_{d_{dr}} = \frac{g}{V_o}\sqrt{K_{n,\beta} + K_{y,\beta}K_{n,\check{r}} + \frac{K_{\ell,\beta}}{K_{\ell,\check{p}}} - \left(K_{\ell,\beta} + K_{y,\beta}K_{\ell,\check{r}}\right)\frac{K_{n,\check{p}}}{K_{\ell,\check{p}}} - \frac{1}{4}\left(K_{y,\beta} + K_{n,\check{r}}\right)^2} \tag{A.38}$$

the terms are redimensionalized as

$$\omega_{d_{dr}} = \frac{g}{V_o}\sqrt{-\frac{V_o^2}{g^2}\frac{Y_{,\beta}}{I_{zz_b}}l_{mp_n} + \frac{V_o^2 \ell_{,\beta}}{g^2 I_{xx_b}}\frac{g I_{xx_b}}{V_o \ell_{,p}} - \frac{V_o^2}{g^2}\frac{Y_{,\beta}}{I_{xx_b}}h_{mp_\ell}\frac{V_o n_{,p}}{g I_{zz_b}}\frac{g I_{xx_b}}{V_o \ell_{,p}} - \frac{1}{4}\left(\frac{V_o Y_{,\beta}}{g I_{zz_b}}a_{zz_b}\right)^2} \tag{A.39}$$

and simplified, as

$$\omega_{d_{dr}} = \sqrt{-\frac{Y_{,\beta}}{I_{zz_b}}\left(l_{mp_n} + h_{mp_\ell}\frac{n_{,p}}{\ell_{,p}} - \frac{Wr^2_{zz_b}h_{np_\ell}}{V_o\ell_{,p}} + \frac{1}{4}\frac{Y_{,\beta}}{I_{zz_b}}a^2_{zz_b}\right)} \tag{A.40}$$

The Dutch-roll natural frequency is found to be

$$\begin{aligned}\omega_{n_{dr}} &= \sqrt{\sigma^2_{dr} + \omega^2_{d_{dr}}} \\ &= \left\{\frac{1}{4}\left[\frac{Y_{,\beta}}{I_{zz_b}}\left(a_{zz_b} + I_{xx_b}\left(\frac{n_{,p}}{\ell^2_{,p}}h_{mp_\ell} - \frac{Wr^2_{zz_b}}{V_o\ell^2_{,p}}h_{np_\ell}\right) - \frac{\ell_{,r}n_{,p}}{Y_{,\beta}\ell_{,p}}\right) + \frac{W}{\ell_{,p}}\left(\frac{h_{mp_\ell}l_{np_n}}{l_{mp_n}} - h_{np_\ell}\right)\right]^2\right. \\ &\qquad \left. - \frac{Y_{,\beta}}{I_{zz_b}}\left(l_{mp_n} + h_{mp_\ell}\frac{n_{,p}}{\ell_{,p}} - \frac{Wr^2_{zz_b}h_{np_\ell}}{V_o\ell_{,p}} + \frac{1}{4}\frac{Y_{,\beta}}{I_{zz_b}}a^2_{zz_b}\right)\right\}^{1/2}\end{aligned} \tag{A.41}$$

The Dutch-roll damping ratio is found as

$$\begin{aligned}\zeta_{dr} &= \frac{\sigma_{dr}}{\sqrt{\sigma^2_{dr} + \omega^2_{d_{dr}}}} \\ &= -\frac{1}{2}\left[\frac{Y_{,\beta}}{I_{zz_b}}\left(a_{zz_b} + I_{xx_b}\left(\frac{n_{,p}}{\ell^2_{,p}}h_{mp_\ell} - \frac{Wr^2_{zz_b}}{V_o\ell^2_{,p}}h_{np_\ell}\right) - \frac{\ell_{,r}n_{,p}}{Y_{,\beta}\ell_{,p}}\right) + \frac{W}{\ell_{,p}}\left(\frac{h_{mp_\ell}l_{np_n}}{l_{mp_n}} - h_{np_\ell}\right)\right] \Bigg/ \\ &\quad \left\{\frac{1}{4}\left[\frac{Y_{,\beta}}{I_{zz_b}}\left(a_{zz_b} + I_{xx_b}\left(\frac{n_{,p}}{\ell^2_{,p}}h_{mp_\ell} - \frac{Wr^2_{zz_b}}{V_o\ell^2_{,p}}h_{np_\ell}\right) - \frac{\ell_{,r}n_{,p}}{Y_{,\beta}\ell_{,p}}\right) + \frac{W}{\ell_{,p}}\left(\frac{h_{mp_\ell}l_{np_n}}{l_{mp_n}} - h_{np_\ell}\right)\right]^2\right. \\ &\qquad \left. - \frac{Y_{,\beta}}{I_{zz_b}}\left(l_{mp_n} + h_{mp_\ell}\frac{n_{,p}}{\ell_{,p}} - \frac{Wr^2_{zz_b}h_{np_\ell}}{V_o\ell_{,p}} + \frac{1}{4}\frac{Y_{,\beta}}{I_{zz_b}}a^2_{zz_b}\right)\right\}^{1/2}\end{aligned} \tag{A.42}$$

Acknowledgments

This work was partially funded by the U.S. Office of Naval Research Sea-Based Aviation program (grant no. N00014-18-1-2502) with Brian Holm-Hansen as the Program Officer. This work was also funded by the Warren F. Phillips student fellowship.

References

[1] Wilhelm, K., "Military Standard-Flying Qualities of Piloted Aircraft," Tech. Rep. MIL-STD-1797, US Air Force Department, 1990.

[2] Cooper, G. E., and Harper, R. P., "The Use of Pilot Rating in the Evaluation of Aircraft Handling Qualities," Tech. Rep. TN D-5153, NASA, 1969.

[3] Harper Jr, R. P., and Cooper, G. E., "Handling Qualities and Pilot Evaluation," *Journal of Guidance, Control, and Dynamics*, Vol. 9, No. 5, 1986, pp. 515–529. https://doi.org/10.2514/3.20142.

[4] Hess, R. A., "Unified theory for aircraft handling qualities and adverse aircraft-pilot coupling," *Journal of Guidance, Control, and Dynamics*, Vol. 20, No. 6, 1997, pp. 1141–1148. https://doi.org/10.2514/2.4169.

[5] Gautrey, J., and Cook, M., "A Generic Control Anticipation Parameter for Aircraft Handling Qualities Evaluation," *The Aeronautical Journal*, Vol. 102, No. 1013, 1998, pp. 151–160. https://doi.org/10.1017/S000192400006543X.

[6] Mavris, D., DeLaurentis, D., and Soban, D., "Probabilistic Assessment of Handling Qualities Characteristics in Preliminary Aircraft Design," *36th AIAA Aerospace Sciences Meeting and Exhibit*, 1998, p. 492. https://doi.org/10.2514/6.1998-492.

[7] Smetana, F. O., Summery, D., and Johnson, W. D., "Riding and Handling Qualities of Light Aircraft: A Review and Analysis," Tech. Rep. CR-1975, NASA, 1972.

[8] Barber, M. R., "An Evaluation of the Handling Qualities of Seven General Aviation Aircraft," Tech. Rep. TN D-3726, NASA, 1966.

[9] van Dam, C. P., Holmes, B. J., and Pitts, C., "Effect of Winglets on Performance and Handling Qualities of General Aviation Aircraft," *Journal of Aircraft*, Vol. 18, No. 7, 1981, pp. 587–591. https://doi.org/10.2514/3.57531.

[10] Hess, R. A., and Joyce, R., "Analytical Investigation of Transport Aircraft Handling Qualities," *AIAA Atmospheric Flight Mechanics (AFM) Conference*, 2013, p. 4505. https://doi.org/10.2514/6.2013-4505.

[11] Foster, T., and Bowman, J., "Dynamic Stability and Handling Qualities of Small Unmanned-Aerial Vehicles," *43rd AIAA Aerospace Sciences Meeting and Exhibit*, 2005, p. 1023. https://doi.org/10.2514/6.2005-1023.

[12] Klyde, D. H., Schulze, P. C., Mitchell, D., and Alexandrov, N., "Development of a Process to Define Unmanned Aircraft Systems Handling Qualities," *2018 AIAA Atmospheric Flight Mechanics Conference*, 2018, p. 0299. https://doi.org/10.2514/6.2018-0299.

[13] Snow, S. A., and Hunsaker, D. F., "Design and Performance of a 3D-Printed Morphing Aircraft," *AIAA SciTech 2021 Forum*, AIAA, Virtual, 2021, p. 1060. https://doi.org/10.2514/6.2021-1060.

[14] Bilimoria, K. D., "Effects of Control Power and Guidance Cues on Lunar Lander Handling Qualities," *Journal of Spacecraft and Rockets*, Vol. 46, No. 6, 2009, pp. 1261–1271. https://doi.org/10.2514/1.40187.

[15] Anderson, S. B., "Historical Overview of V/STOL Aircraft Technology," Tech. Rep. TM-81280, NASA, 1981.

[16] Phillips, W. H., "Flying Qualities from Early Airplanes to the Space Shuttle," *Journal of Guidance, Control, and Dynamics*, Vol. 12, No. 4, 1989, pp. 449–459. https://doi.org/10.2514/3.20432.

[17] Mitchell, D. G., Doman, D. B., Key, D. L., Klyde, D. H., Leggett, D. B., Moorhouse, D. J., Mason, D. H., Raney, D. L., and Schmidt, D. K., "Evolution, Revolution, and Challenges of Handling Qualities," *Journal of Guidance, Control, and Dynamics*, Vol. 27, No. 1, 2004, pp. 12–28.

[18] Klyde, D. H., Aponso, B. L., Mitchell, D. G., and Latimer, K. J., "Development of demonstration maneuvers for aircraft handling qualities evaluation," *22nd Atmospheric Flight Mechanics Conference*, 1997, p. 3653. https://doi.org/10.2514/6.1997-3653.

[19] Hess, R., "Investigating Aircraft Handling Qualities using a Structural Model of the Human Pilot," *Guidance, Navigation and Control Conference*, 1987, p. 2537. https://doi.org/10.2514/6.1987-2537.

[20] Shevell, R. S., *Fundamentals of flight*, Prentice-Hall Inc., 1983.

[21] McCormick, B. W., *Aerodynamics, Aeronautics, and Flight Mechanics*, 2nd ed., Wiley, New York, 1994.

[22] Barnard, R. H., and Philpott, D. R., *Aircraft flight: a description of the physical principles of aircraft flight*, 3rd ed., Pearson education, 2004.

[23] Torenbeek, E., and Wittenberg, H., *Flight Physics: Essentials of Aeronautical Disciplines and Technology, with Historical Notes*, Springer Science & Business Media, 2009.

[24] Kundu, A. K., *Aircraft Design*, Cambridge University Press, 2010.

[25] Kolk, W. R., *Modern Flight Dynamics*, Prentice Hall, Inc., 1961.

[26] Seckel, E., *Stability and Control of Airplanes and Helicopters*, Academic Press Inc., 1964.

[27] McRuer, D., Ashkenas, I., and Graham, D., "Aircraft Dynamics and Automatic Control," Tech. Rep. 129-1, Nava Air Systems Command, 1968.

[28] McRuer, D. T., Ashkenas, I., and Graham, D., *Aircraft Dynamics and Automatic Control*, Princeton University Press, 1973.

[29] Abbott, I. H., and Doenhoff, A. E. V., "Families of Wing Sections," *Theory of Wing Sections*, McGraw–Hill, New York, 1949, (republished by Dover, New York, 1959), Chap. 6, pp. 111–123.

[30] Blakelock, J. H., *Automatic Control of Aircraft and Missiles*, 2nd ed., John Wiley & Sons, 1991.

[31] Cook, M. V., *Flight Dynamics Principles*, John Wiley & Sons, Inc., 1997.

[32] Schmidt, L. V., *Introduction to Aircraft Flight Dynamics*, AIAA, 1998.

[33] Yechout, T. R., *Introduction to Aircraft Flight Mechanics*, AIAA, 2000.

[34] Stengel, R. F., *Flight Dynamics*, 2nd ed., Princeton University Press, 2022.

[35] Raol, J. R., and Singh, J., *Flight Mechanics Modeling and Analysis*, CRC Press, 2009.

[36] Phillips, W. F., *Mechanics of Flight*, 2nd ed., John Wiley & Sons, Inc., 2010.

[37] Teper, G. L., "Aircraft Stability and Control Data," Tech. Rep. CR-96008, NASA, 1969.

[38] Heffley, R. K., and Jewell, W. F., "Aircraft Handling Qualities Data," Tech. Rep. CR-2144, NASA, 1972.

[39] Phillips, W. F., "Longitudinal Static Stability and Trim : Stick-Fixed Neutral Point and Static Margin," *Mechanics of Flight*, John Wiley & Sons, Inc., 2010, Chap. 4, 2nd ed., pp. 400–411.

[40] Phillips, W., and Niewoehner, R., "Characteristic Length and Dynamic Time Scale Associated with Aircraft Pitching Motion," *Journal of Aircraft*, Vol. 46, No. 2, 2009, pp. 572–582. https://doi.org/10.2514/1.38724.

[41] Phillips, W. F., "Aircraft Controls and Maneuverability : Longitudinal Control and Maneuverability," *Mechanics of Flight*, John Wiley & Sons, Inc., 2010, Chap. 6, 2nd ed., pp. 715–725.

[42] Phillips, W. F., "Linearized Longitudinal Dynamics : Short-Period Approximation," *Mechanics of Flight*, John Wiley & Sons, Inc., 2010, Chap. 8, 2nd ed., pp. 847–854.

[43] Phillips, W. F., "Linearized Longitudinal Dynamics : Long-Period Approximation," *Mechanics of Flight*, John Wiley & Sons, Inc., 2010, Chap. 8, 2nd ed., pp. 854–871.

[44] Phillips, W. F., "Linearized Lateral Dynamics : Roll Approximation," *Mechanics of Flight*, John Wiley & Sons, Inc., 2010, Chap. 9, 2nd ed., pp. 896–897.

[45] Phillips, W. F., "Linearized Lateral Dynamics : Spiral Approximation," *Mechanics of Flight*, John Wiley & Sons, Inc., 2010, Chap. 9, 2nd ed., pp. 897–905.

[46] Phillips, W. F., "Linearized Lateral Dynamics : Dutch Roll Approximation," *Mechanics of Flight*, John Wiley & Sons, Inc., 2010, Chap. 9, 2nd ed., pp. 906–922.

[47] Hunsaker, D. F., and Moulton, B. C., "An Alternate Dimensionless Form of the Linearized Rigid-Body Aircraft Equations of Motion with Emphasis on Dynamic Parameters," *AIAA SciTech 2023 Forum*, 2023, p. 1366. https://doi.org/10.2514/6.2023-1366.

[48] Bihrle Jr, W., "A Handling Qualities Theory for Precise Flight-Path Control," Tech. Rep. AFFDL-TR-65-198, Air Force Flight Dynamics Laboratory, 1966.

[49] Bolander, C. R., Kohler, A. J., Hunsaker, D. F., Myszka, D., and Joo, J. J., "Static Trim of a Bio-Inspired Rotating Empennage for a Fighter Aircraft," *AIAA SciTech 2023 Forum*, 2023, p. 0624. https://doi.org/10.2514/6.2023-0624.

[50] Etkin, B., *Dynamics of Atmospheric Flight*, John Wiley & Sons, Inc., 1972.

[51] Cook, M. V., "Flying and Handling Qualities," *Flight Dynamics Principles*, John Wiley & Sons, Inc., 1997, pp. 203–233.

[52] Smith, R. H., "A Theory for Longitudinal Short-Period Pilot Induced Oscillations." Tech. Rep. AFFDL-TR-77-57, Air Force Flight Dynamics Laboratory, 1977.

[53] Phillips, W. F., "Aircraft Equations of Motion : Rigid-Body 6-DOF Equations of Motion," *Mechanics of Flight*, John Wiley & Sons, Inc., 2010, Chap. 7, 2nd ed., pp. –.

[54] Phillips, W. F., "Aircraft Controls and Maneuverability : Lateral Control and Maneuverability," *Mechanics of Flight*, John Wiley & Sons, Inc., 2010, Chap. 6, 2nd ed., pp. 666–679.

[55] of Defense, U. S. D., "Military Specification - Flying Qualities of Piloted Airplanes," Tech. Rep. MIL-F-8785C, United States Department of Defense, 1980.

[56] Etkin, B., "Stability of Steady Flight," *Dynamics of Atmospheric Flight*, John Wiley & Sons, Inc., 1972, pp. 319–399.

[57] Stengel, R. F., "Longitudinal Motions," *Flight Dynamics*, Princeton University Press, 2022, 2nd ed., pp. 395–487.

[58] Torenbeek, E., and Wittenberg, H., "Stability and Control," *Flight Physics: Essentials of Aeronautical Disciplines and Technology, with Historical Notes*, Springer Science & Business Media, 2009, pp. 327–403.

[59] Phillips, W. F., "Aircraft Handling Qualities and Control Response : Dynamic Handling Quality Prediction," *Mechanics of Flight*, John Wiley & Sons, Inc., 2010, Chap. 10, 2nd ed., pp. 958–968.

[60] Schmidt, L. V., "Longitudinal Dynamics," *Introduction to Aircraft Flight Dynamics*, AIAA, 1998, pp. 165–206.

[61] Nelson, R. C., "Longitudinal Motion (Stick Fixed)," *Flight Stability and Automatic Control*, McGraw-Hill, Inc., 1989, pp. 112–151.

[62] Cook, M. V., "Longitudinal Dynamics," *Flight Dynamics Principles*, John Wiley & Sons, Inc., 1997, pp. 113–144.

[63] Kolk, W. R., "Longitudinal Motion," *Modern Flight Dynamics*, Prentice Hall, Inc., 1961, pp. 69–86.

[64] McRuer, D. T., Ashkenas, I., and Graham, D., *Longitudinal Dynamics*, Princeton University Press, 1973.

[65] Yechout, T. R., "Aircraft Dynamic Stability," *Introduction to Aircraft Flight Mechanics*, AIAA, 2000, pp. 303–387.

[66] Nelson, R. C., "Lateral Motion (Stick Fixed)," *Flight Stability and Automatic Control*, McGraw-Hill, Inc., 1989, pp. 152–175.

[67] Cook, M. V., "Lateral-Directional Dynamics," *Flight Dynamics Principles*, John Wiley & Sons, Inc., 1997, pp. 145–176.

[68] Raol, J. R., and Singh, J., "Simplification of Equations of Motion and Transfer-Function Analysis," *Flight Mechanics Modeling and Analysis*, CRC Press, 2009, pp. 121–158.

[69] Kolk, W. R., "Flying Qualities," *Modern Flight Dynamics*, Prentice Hall, Inc., 1961, pp. 122–149.

[70] Schmidt, L. V., "Lateral-Directional Dynamics," *Introduction to Aircraft Flight Dynamics*, AIAA, 1998, pp. 207–256.

[71] Ellis, D. R., and Seckel, E., "Flying Qualities of Small General Aviation Airplanes. Part 1. The Influence of Dutch-Roll Frequency, Dutch-Roll Damping, and Dihedral Effect," Tech. Rep. DS-69-8, Federal Aviation Administration, 1969.

[72] Gamble, L. L., and Smith, C. W. L., "Improved Dutch Roll Stability Augmentation System for a Modified C-135B Aircraft," Master's thesis, Air Force Institute of Technology, 1970.

[73] Goslin, T., Ansari, F., and Chakravarty, A., "An Optimized Yaw Damper for Enhanced Passenger Ride Comfort," *1987 American Control Conference*, IEEE, 1987, pp. 395–396. https://doi.org/10.23919/ACC.1987.4789350.

[74] Gennarelli, T. A., Thibault, L. E., Tomei, G., Wiser, R., Graham, D., and Adams, J., "Directional Dependence of Axonal Brain Injury Due to Centroidal and Non-Centroidal Acceleration," *SAE Transactions*, 1987, pp. 1355–1359.